P-08-07

Oskarshamn site investigation

Structural characterisation of deformation zones (faults and ductile shear zones) from selected drill cores from the Laxemar area

Giulio Viola, Guri Venvik Ganerød
Geological Survey of Norway, N-7491 Trondheim, Norway

December 2007

Svensk Kärnbränslehantering AB
Swedish Nuclear Fuel
and Waste Management Co
Box 250, SE-101 24 Stockholm
Tel +46 8 459 84 00

ISSN 1651-4416
SKB P-08-07

Oskarshamn site investigation

Structural characterisation of deformation zones (faults and ductile shear zones) from selected drill cores from the Laxemar area

Giulio Viola, Guri Venvik Ganerød
Geological Survey of Norway, N-7491 Trondheim, Norway

December 2007

Keywords: Oskarshamn, AP PS 400-07-016, Structural geology, Shear zone, Fault, Fault rocks, Kinematics.

Abstract

A study of predominantly brittle structures, i.e. brittle deformation zones, faults, fractures and associated fault rocks, was carried out on a number of drill cores from the Laxemar area, Oskarshamn. The main aim of the study was to document from a geometric and kinematic point of view the brittle deformational history of the region. The study deals with the detailed characterization of the observed deformation zones and fault rocks were systematically investigated in order to improve our understanding of the deformation mechanisms that controlled the local brittle structural evolution. Striated surfaces were used to constrain the kinematics of fault zones.

Deformation zone (DZ) 7 of core **KLX13A** is a long and complex deformation zone, which differs from a "typical" deformation zone in that it lacks a single and well-defined fault core containing fault rocks and the associated transition zones. DZ 7 is instead characterised by very pervasive sets of fractures, which lead to volumetrically significant crush zones and core loss intervals. Remarkable fault rock intervals are observed at different depths within the DZ. Given the high spatial frequency of this type of brittle features (and the impossibility to subdivide the logged interval into individual and distinct, meaningful cores and transition zones) we assign almost the entire logged depth interval to a single DZ core. Between the numerous crush zones and core loss intervals there are metres of intact host rock, probably reflecting the anastomosing geometry of the deformation zone.

DZ 16 and 20 were logged in core **KLX15A**. DZ 16 contains little pervasive deformational features and is not classified as a proper deformation zone. In fact, long sections of it are made of by basically undeformed quartzmonzonites without any evidence of significant structural overprinting. DZ 20 is not covered by borehole images. It is characterised by a core containing an early ductile fabric overprinted by brittle deformation that generated protocataclasites and cataclasites, with a very high fracture frequency, leading to crush zones and localized core loss.

DZ 12 in core **KLX16A** contains several minor and very thin brittle fault cores, decorated by spectacular cataclasite-ultracataclasite/cemented breccias. Core loss intervals are commonly observed.

Two deformation zones (DZ 1 and DZ 3) were logged in core **KLX17A**. DZ 1 is primarily characterised by a c. 3 m thick core. Large cavities in the corresponding borehole image suggest the core to be a zone of extreme mechanical weakness.

DZ 3 is developed in porphyritic granites, quartz monzodiorites and diorites. Its main structural feature is a series of brittle fault cores at different depths. These are characterised by cataclastic cores and dense sealed networks of fine-grained epidote veins and associated dilation/cataclasis. Several striated planes were constrained kinematically within DZ 3; there are sets of NW- and SE-dipping reverse and normal shear fractures and a group of much steeper SE-NW-striking and SW-dipping shear fractures with a component of sinistral and dextral oblique shear.

DZ 4 in core **KLX19A** contains several thin ENE-WSW-trending fault cores with no or only minor transition zones. Some ductile precursors are locally observed. Brittle fault cores are here defined on the basis of high fracture frequencies rather than on the presence of fault rock.

DZ 5 is entirely hosted by a dolerite dyke intruding quartz monzonites. The fracture frequency increases significantly within the mafic intrusion up to values well in excess of 9 f/m, which warrants the establishment of a DZ core within the dyke. A systematically observed geometric relationship shows low α, steep fractures, usually arranged in anastomosing sealed networks, crosscut by high-α flatter fractures. Normal kinematics were documented for some of the gently dipping fractures.

DZ 6 does not contain any relevant structural feature and is therefore not classified as a deformation zone.

DZ 7 is entirely located within a doleritic dyke. The dolerite contains a high fracture density that locally leads to narrow crash zones and minor intervals of core loss. Neither ductile features nor fault rocks were observed. The granitic host rock contains distinctly less fractures than the dolerite.

DZ 12 of core **KLX21B** contains no significant structural features and is therefore not interpreted as a proper deformation zone

Sammanfattning

Et undersøkelse av overveiende sprø strukturer, dvs sprø deformasjonssoner, forkastninger, brudd og tilhørende forkastningsbergarter, er utført på flere borekjerner fra Laxemar-området, Oskarshamn. Hovedformålet med undersøkelsen er fra et geometrisk og kinematisk synspunkt å dokumentere den sprø deformasjonshistorien i området. Undersøkelsen omfatter detaljert karakterisering av de observerte deformasjonssonene. Forkastningsbergarter ble systematisk undersøkt for å forbedre forståelsen av deformasjonsmekanismene som kontrollerte den lokale sprø utviklingen av strukturene. Overflater med glidestriper ble brukt for å bestemme kinematikken til forkastningssonene.

DZ (deformasjonssone) 7 fra borkjerne **KLX13A** er en lang og kompleks deformasjonssone som skiller seg fra en ”typisk” deformasjonssone fordi den mangler en veldefinert forkastningskjerne med forkastningsbergarter og de tilhørende overgangssoner. DZ 7 er i stedet karakterisert av gjennomsettende sett med bruddsoner, som fører til betydelige mengder av knusningssoner og kjernetap. Spesielle områder med forkastningsbergarter er observert på forskjellige dyp i deformasjonssonen. Tatt i betraktning den høye frekvensen av denne type sprø elementer (og det faktum at det er umulig å inndele det loggede intervall i individuelle, distinkte og meningsfulle kjerner og overgangssoner) så har vi klassifisert nesten hele det loggede dybdeintervallet til en enkel DZ kjerne. Mellom de tallrike knusningssonene og kjernetapene er det noen meter med intakt opprinnelig bergart som trolig reflekterer den anastomoserende (nettverkslignende) geometrien til deformasjonssonen.

DZ16 og 20 ble logget i **KLX15A**. DZ 16 inneholder få gjennomsettende deformasjonstrekk og er ikke klassifisert som en ekte deformasjonssone. Lange stykker består hovedsaklig av udeformerte kvartsmonzonitter uten betydelig strukturell overpreging. DZ 20 er ikke dekket av borehullsbilder. Den er karakterisert av en kjerne som inneholder en tidlig duktil struktur som er overpreget av en sprø deformasjon. Denne danner protoklastitter og kataklastitter med en svært høy bruddfrekvens, noe som fører til knusningssoner og kjernetap.

DZ 12 fra **KLX16A** inneholder flere mindre og svært tynne sprø forkastningskjerner som er omgitt av iøynefallende kataklastitt-ultrakataklastitt-sementerte breksjer. Områder med kjernetap er ofte observert.

To deformasjonssoner (DZ 1 og DZ 3) ble logget i **KLX17A**. DZ 1 er først og fremst karakterisert av en ca. 3m tykk kjerne. Store hulrom i det tilhørende borehullsbildet antyder at kjernen ligger i en sone med ekstrem mekanisk svakhet.

DZ3 er utviklet i porfyrittiske granitter, kvarts-monzodioritter og dioritter. Dens strukturelle hovedtrekk er en serie med sprø forkastningskjerner på forskjellige dyp. Disse er karakterisert ved kataklastiske kjerner og tette forseglete nettverk av finkornede epidot-årer og tilhørende utvidelse/kataklase. Flere stripningsplan ble bestemt kinematisk i DZ 3 og representerer sett med NV- og SØ-fallende revers og normal forkastninger, og en gruppe steilere SØ-NV-strykende og SV-fallende brudd med komponenter av venstrelengs og høyrelengs skrå skjærbevegelser.

DZ 4 i **KLX19A** inneholder flere ØNØ-VNV strykende forkastningskjerner med ingen eller få overgangssoner. Noen områder med begynnende duktil deformasjon er observert. Sprø forkastningskjerner er her definert på basis av høy bruddfrekvens snarere enn tilstedeværelse av forkastningsbergarter.

DZ 5 er lokalisert i en dolerittgang som intruderer kvarts-monzonitt. Bruddfrekvensen øker betydelig innenfor den mafiske intrusjonen opp til verdier som overstiger 9 brudd/m, noe som rettferdiggjør etableringen av en DZ-kjerne innenfor gangen. Et systematisk observert geometrisk forhold viser lav α, steile brudd, vanligvis arrangert in et amamostoserende (nettverkslignende) forseglet mønster, gjennomsatt av brudd med flatere høy-α. Normal kinematikk ble dokumentert i noen av de slakt fallende bruddene.

DZ 6 inneholder ingen relevante strukturelementer og er derfor ikke klassifisert som en deformasjonssone.

DZ 7 er fullstendig lokalisert innenfor en dolerittgang. Doleritten inneholder en høy bruddtetthet som lokalt fører til tynne knusningssoner og mindre områder med kjernetap. Verken duktile soner eller forkastningsbergarter ble observert. Den granittiske vertsbergarten inneholder betydelig færre brudd enn doleritten.

DZ 12 fra **KLX 21B** inneholder ingen betydelige strukturelementer og er derfor ikke tolket som en ekte deformasjonssone.

Contents

1 Introduction

This report provides the detailed characterisation, in terms of deformation characteristics, geometry and, when possible, kinematics of selected brittle deformation zones at the Oskarshamn investigation site (Figure 1-1). This report forms the continuation of two similar studies by the same authors /Viola and Venvik Ganerød 2007ab/. Detailed logging and structural characterisation were performed on several depth intervals from a series of chosen drill cores, selected for their complexity and for the structural relevance of the deformation zones (from here on referred to as "DZ" and identified as such in the geological single-hole interpretation studies) they intersected.

This study forms one of the activities performed within the site investigation process at Oskarshamn. The work was carried out in accordance with activity plan AP PS 400-07-016. Controlling documents for performing this activity are listed in Table 1-1. Both activity plan and method descriptions are SKB internal controlling documents.

Table 1-1. Controlling documents for the performance of the activity.

Activity Plan	**Number**	**Version**
Name	AP PS 400-07-016	1.0
Method Descriptions	**Number**	**Version**
/Braathen 1999/	Tectonophysics 302, 99–121.	
/Braathen et al. 2002/	Norwegian Journal of Geology, 82, 225–241.	
/Braathen et al. 2004/	Tectonics, 23, TC4010, doi:10.1029/2003TC001558.	
/Munier et al. 2003/	SKB R-03-07	
/Nordgulen et al. 2002/	Norwegian Journal of Geology, 82, 299–316.	
/Osmundsen et al. 2003/	Journal of the Geological Society, London 160, 1–14.	
/Petit 1987/	Journal of Structural Geology 9, 597–608.	

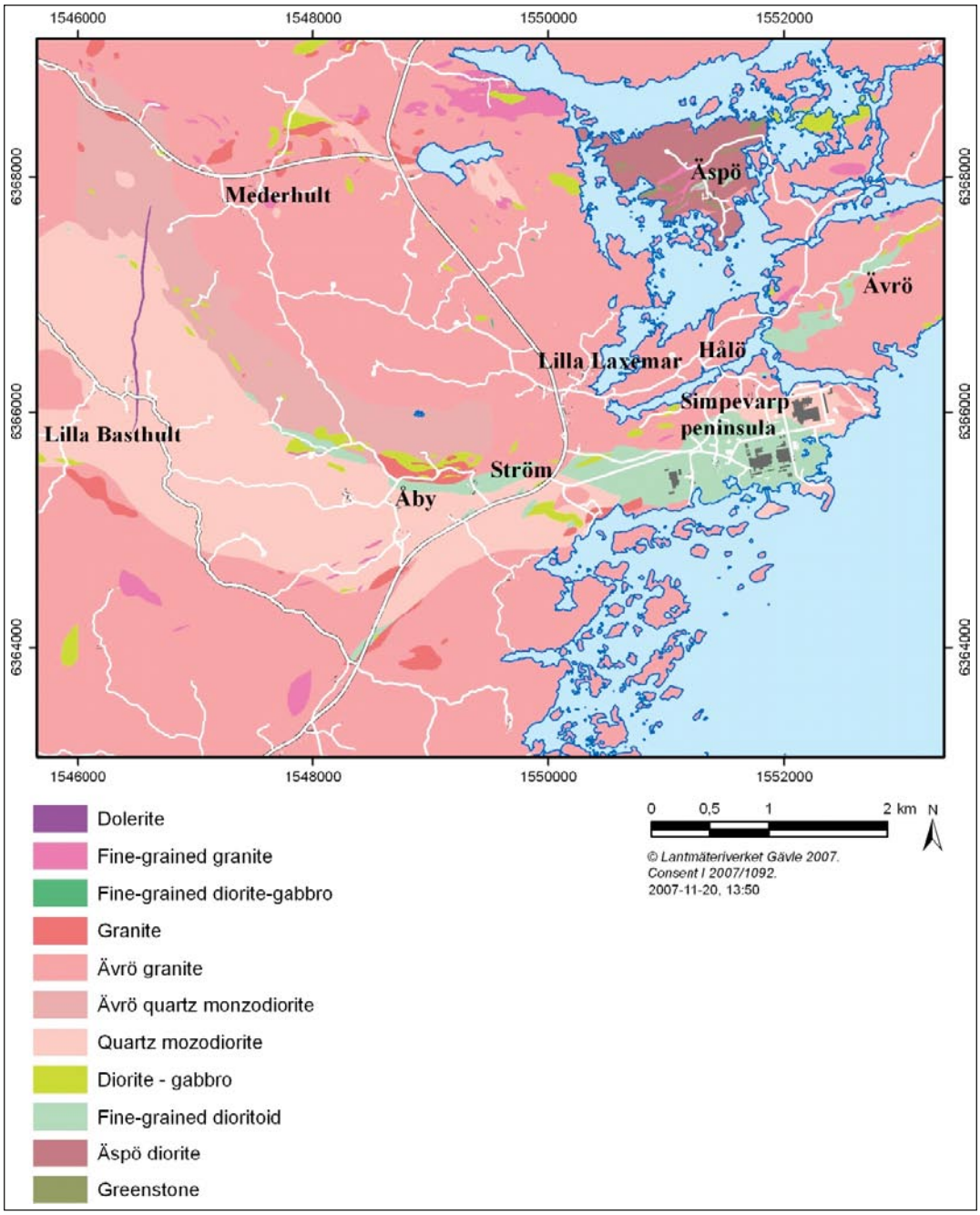

Figure 1-1. *Geology map of the Oskarshamn site investigation area.*

2 Objective and scope

The aim of this study was to document, describe and characterise structurally, by means of detailed geometric and kinematic analyses, a number of predominantly brittle deformation zones from selected drill cores. Fault rocks associated with these deformation zones, when present, were also studied in order to improve our understanding of the deformation mechanisms that controlled the local deformation history. Data from drill cores, combined with observations from selected thin sections, form the basis for the results and conclusions of this study.

3 Equipment

3.1 Description of equipment/interpretation tools

During the drill core logging phase we used the standard equipment for structural investigations, including hammer, compass, hand lens, diluted HCl and digital camera. Samples collected from the cores were cut in the core laboratory, and selected oriented slabs were marked and sent in for preparation of polished thin sections.

4 Execution

4.1 Methodology

The standard procedure for obtaining the true orientation of linear structures (lineations, striations, etc) on fault surfaces in drill cores with known orientation is as follows:

1. Fractures of potential interest were identified by visual inspection of drill cores from selected deformation zones, as defined previously by the geological single hole interpretations.
2. Individual fractures were identified on the BIPS image of the borehole wall, which provides a mirror image of the core itself. Care had to be taken to ensure that the fracture selected on the image matched the one from the drill core. In some cases this was challenging, particularly where abundant fractures cut the core at different angles. Independent checks that the correct fracture was chosen could be carried out by using information contained in the drill core database, as, for example, the properties of the fracture itself, the acute angle α between the fracture and the core axis, and the angle β, which is the angle (measured counter-clockwise) from the lower intersection of the fracture with the core wall, to the top of the drill core.
3. Having identified the fracture of interest, the top of the drill core was marked based on visual inspection of the BIPS image and on the angle β. The fractures orientation (strike and dip) was obtained using the information contained in the drill core database.
4. The core was positioned the right way up and at the true inclination using a core holder supplied by SKB. This device allowed the accurate adjustment of the core inclination as given in the database.
5. The orientation of the linear structure was determined by measuring its trend and plunge.
6. Once the sense of slip was determined with confidence, the true movement of the hanging wall with respect to the footwall of the fault was established.
7. Relevant data were recorded in a database.

Thin section samples were collected from some of the drill cores. Polished sections were studied at the Geological Survey of Norway (Trondheim) using standard petrographic techniques.

4.2 General

Literature studies preceded the investigations, which were carried out at the Oskarshamn core-logging facility on June 25–29 2007 for a total of five working days.

The following drill cores and relative deformation zones were inspected during this study:

Drill core	Logged length (m)	Deformation zone
KLX13A	487–594	DZ 7
KLX15A	706–744	DZ 16
	976–1,000	DZ 20
KLX16A	325–435	DZ 12
KLX17A	98–114	DZ 1
	191–228	DZ 3
KLX19A	436–465	DZ 4
	481–508	DZ 5
	511–553	DZ 6 and 7
KLX21B	594–707	DZ 12
Total:	543 m	

4.3 Data handling and processing

Structural data were analysed at the Geological Survey of Norway (NGU) in Trondheim and plotted using the commercial package Tectonics FP.

Thin sections were analysed in several steps:

1) Scanning at high resolution of the entire section using a standard slide scanner.
2) Printing of the scanned jpg-images as A4 colour prints in order to aid in establishing general structural and textural relationships and to locate critical sites for further detailed microscopic study.
3) Petrographic analysis and documentation of textural and micro-structural relationships using a petrographic microscope and a digital camera attached to it.

4.4 Analysis and interpretation

The working methods used are described in /Braathen 1999, Braathen et al. 2002, Nordgulen et al. 2002, Osmundsen et al. 2003/. In this report, the definition of fault rocks follows the classification scheme of /Braathen et al. 2004/. Criteria for identifying kinematic indicators in the brittle regime are presented, for example, in /Petit 1987/.

A systematic analysis of fault slip data at the micro- and meso-scale has been made aiming at an improved understanding of the kinematic history in the area of interest. The approach consists in the analysis of strike and dip of fault planes and of azimuth and plunge of their striations. This allows the determination of the complete kinematics of fault trends (even major fault trends). It also provides the basis for paleo-stress inversion calculations that can aim at the reconstruction of the stress field evolution through time. Figure 4-1 provides the key to read the conventions used in the stereonets to represent the orientation and the kinematics of individual fault plane/striation pairs.

4.5 Nonconformities

No nonconformities have been noted.

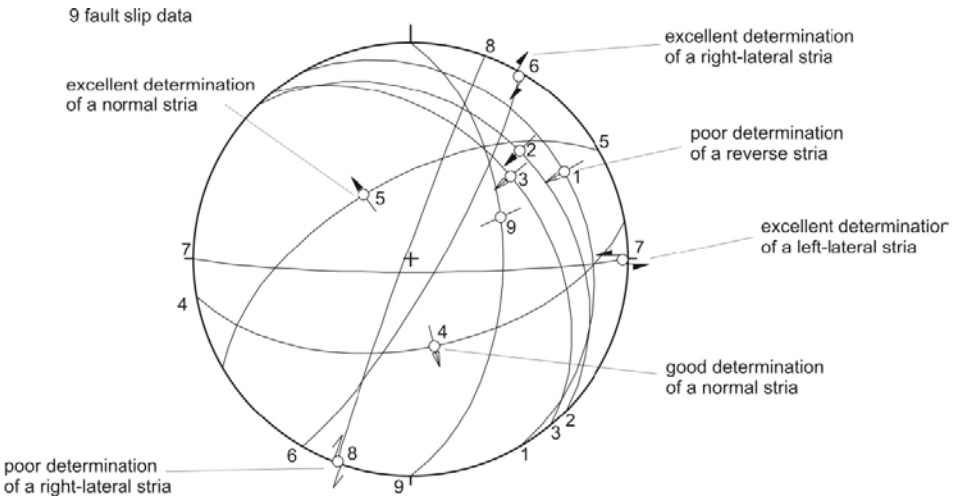

Figure 4-1. *Example of a stereonet plotting kinematic information for striated fault planes (Schmidt projection, lower hemisphere). Keys for striae: outward-directed arrow: normal striation (numbers 4 and 5 on the stereonet); inward directed arrow: reverse striation (numbers 1, 2 and 3); couple of arrows: strike-slip striation (numbers 6, 7 and 8); full black arrowhead: excellent constraints on the sense of shear (numbers 2, 5, 6 and 7); empty arrowhead: good constraints on the sense of shear (numbers 3 and 4); open arrowhead: poor constraints on the sense of shear (numbers 1 and 8); thin line without any arrowhead: no constraints on the sense of shear (number 9).*

4.6 Fault architecture and nomenclature

Faults occur on all scales in the lithosphere. They control the spatial arrangement of rock units, affect the topography, control the permeability of rocks and sediments and, more importantly, accommodate deformation (strain, plus rotation plus translation) during plate interaction and intraplate movements. The term fault zone is generally used for brittle structures in which loss of continuity and slip occurs on several discrete faults within a band of definable width. Shear zones, on the other hand, are ductile structures, across which a rock body does not lose continuity so that strain is progressively distributed across a band of definable width. Based on this definition, a fault zone is a volume of rock where strain is highly localized.

Commonly fault zones can be subdivided into a series of distinctive constituent elements (Figure 4-2 and Figure 4-3). These are 1) the *undeformed host rock*, 2) the *transition zone* /Munier et al. 2003/ (corresponding to the "damage zone" of e.g. /Gudmundsson et al. 2001/) and 3) the proper *fault core* /e.g. Caine et al. 1996, Evens et al. 1997, Braathen and Gabrielsen 2000/. The host rock consists of undeformed rock with low fracture frequency of < 4 fractures/m /Munier et al. 2003/ (Figure 4-2). The transition zone still contains undeformed rock, but the fracture frequency generally increases up to 9 fractures/m (Figure 4-2). Narrow zones or bands of fault rock may occur, especially closer to the boundaries to the fault core. The width of the transition zone varies with the size of the fault zone and the style of deformation, and can range from a few metres to tens of metres. The fault core is identified by the occurrence of fault rock or intensively fractured rock (Figure 4-2 and Figure 4-3). Fault rocks may occur in lenses alternating with pods of relatively undeformed rock /Caine et al. 1996, Braathen and Gabrielsen 2000/. The width of the fault core may vary from cm to m /Braathen and Gabrielsen 2000/.

Rocks that occur within fault zones provide primary evidence for the deformational processes that have occurred there. It is therefore of great importance to fully characterise fault rock occurrences, so as to better understand faulting processes and mechanisms at all scales. Fault rocks form in response to strain localization within fault and shear zones and reflect the interplay of a variety of physical and environmental parameters such as, for example, the finite amount of strain, lithology, style of deformation (i.e. frictional or plastic flow), presence or absence of fluids, strain rate, temperature, pressure and so on. Figure 4-4 reports the classification scheme proposed by /Braathen et al. 2004/ that is adopted in this study to classify fault rock occurrences.

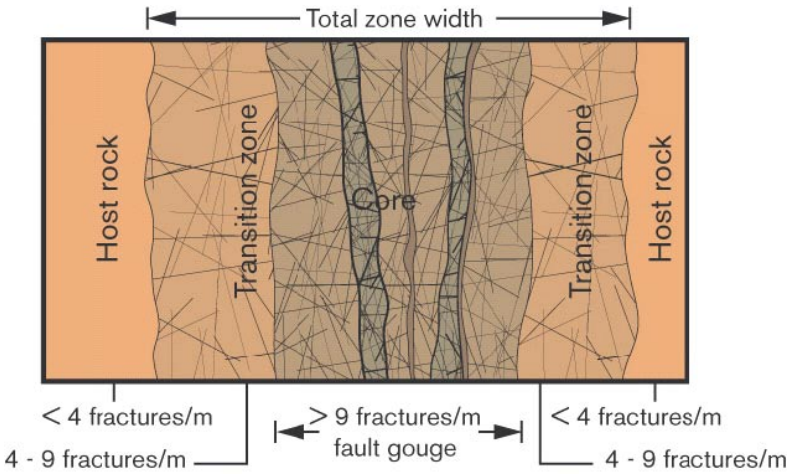

Figure 4-2. *Schematic illustration of a brittle deformation zone according to SKB definition /after Munier et al. 2003/.*

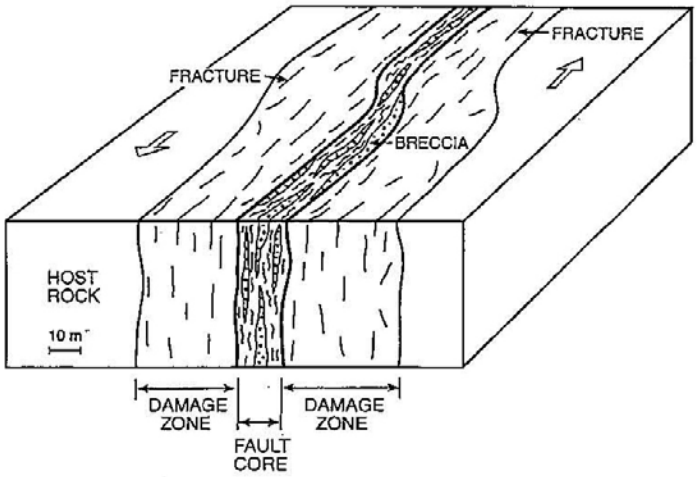

Figure 4-3. *Schematic illustration of the architecture of an idealized fault zone /Gudmundsson et al. 2001/. Note that the term "damage zone" used in this scheme corresponds conceptually to the term "transition zone" of Figure 4-2.*

Brittle ← *Deformation style* → **Ductile**									
Frictional flow ← *Dominant deformation mechanism* → **Plastic flow**									
Non-cohesive			Secondary cohesion		Primary cohesion				*% matrix and grain-size*
			Cemented HB	Indurated HB			*> 50% phyllosilicate*	*< 50% phyllosilicate*	
Hydraulic breccia (HB)	Breccia series	Proto-breccia	Cemented proto-breccia	Indurated proto-breccia	Cataclasite series	Proto-cataclasite	Proto-phyllonite	Proto-mylonite	*0-50% matrix*
		Breccia	Cemented breccia	Indurated breccia		Cataclasite	Phyllonite	Mylonite	*50-90% matrix*
		Ultra-breccia	Cemented ultra-breccia	Indurated ultra-breccia		Ultra-cataclasite	Ultra-phyllonite	Ultra-mylonite	*90-100% matrix*
		Gouge	Cemented gouge	Indurated gouge					*Sub-microscopic matrix*
			Pseudotachylyte						

Blastomylonite

Figure 4-4. *Fault rock classification scheme proposed by /Braathen et al 2004/.*

5 Drill core investigations

In the following section we describe the character and the structural features of the studied deformation zones, with particular emphasis on the occurrence of fault cores and associated fault rocks, transition zones and systematic sets of sealed and open fracture networks. When possible, the sense of shear along striated planes was established in order to add kinematic constraints to the brittle evolution of the area. Observed crosscutting relationships between fractures and faults with different orientations and mineral infill are pointed out, thus providing tighter constraints on the comprehensive understanding of the geological history of the investigation area. The kinematic data are described in relation to the mineralogy of the faults and fractures. The location of the cores investigated in this study is shown in Figure 5-1.

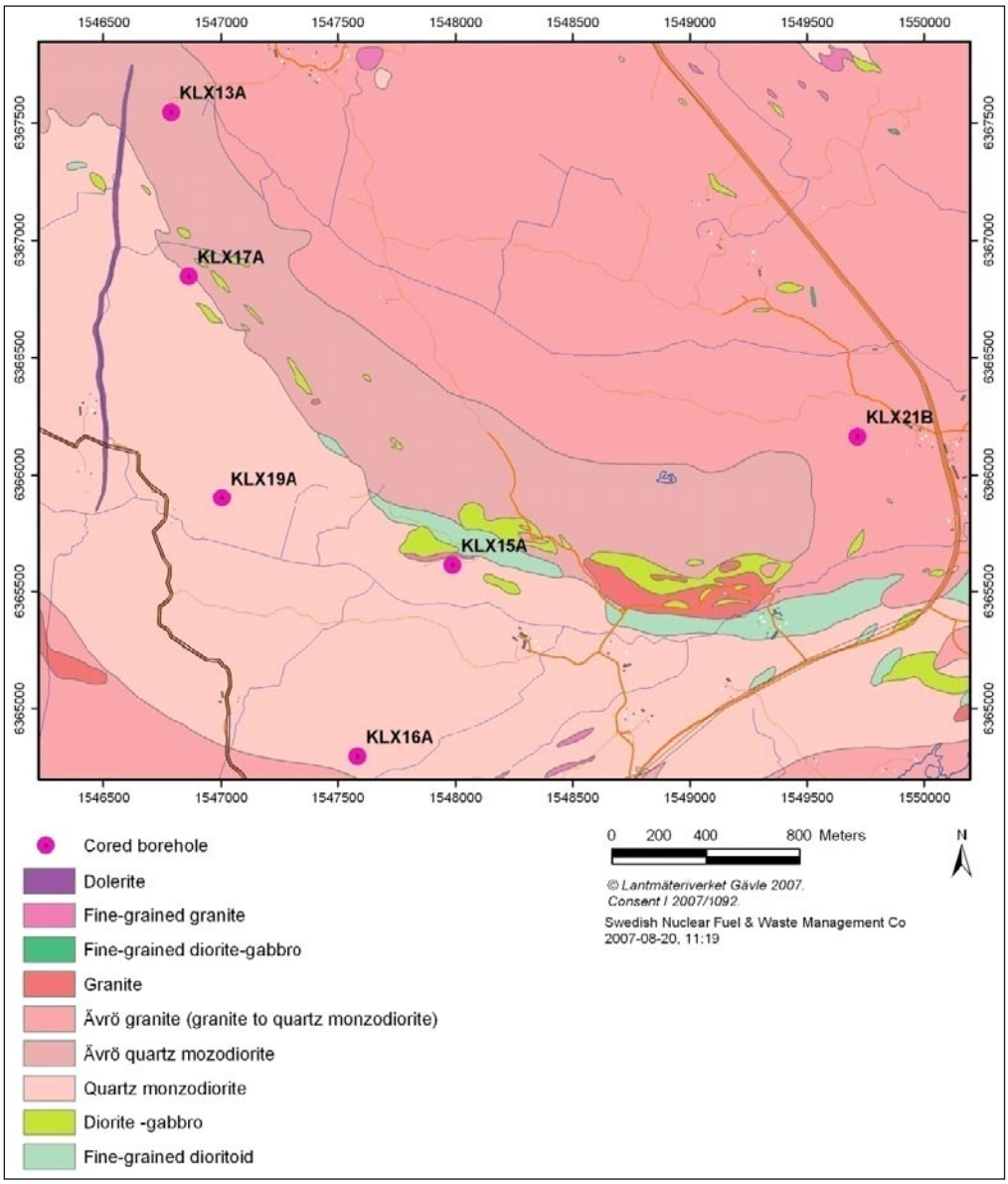

Figure 5-1. *Location of the drill cores described in this report.*

5.1 KLX13A

The drilling site of KLX13A is located in the northern part of the Laxemar area. Ävrö quartz monzodiorites crop out at the surface (Figure 5-1). We have logged DZ 7 (487–594 m). The drill core has a total length of 594 m and is oriented 229/83 within the investigated depth interval /Carlsten et al. 2007a/.

5.1.1 DZ 7: Depth interval 487–594 m

DZ 7 of KLX13A is a long and complex deformation zone, which differs from a "typical" deformation zone due to the lack of a single and well-defined fault core containing fault rocks and the associated transition zones. DZ 7 is instead characterised by very pervasive sets of fractures, which lead to volumetrically significant crush zones and core loss intervals (Figure 5-2). Remarkable fault rock intervals are observed at different depths within the DZ. Given the high spatial frequency of this type of brittle features (and the impossibility to subdivide the logged interval into individual and distinct, meaningful cores and transition zones) we assign almost the entire logged depth interval (490 to 594 m) to a single, yet rather heterogeneous DZ core. Red staining is generally very pervasive throughout DZ 7. Between the numerous crush zones and core loss intervals there are metres of intact host rock, probably reflecting the anastomosing geometry of the deformation zone, a structural feature commonly seen in fault zones.

In the following section we characterise the DZ most significant components.

The upper transition zone of the DZ is very thin; it extends from 487.097 down to 490.770 m depth and is defined by a progressive increase in the fracture frequency with depth and by a c. 19 cm thick crush zone at its upper boundary.

The DZ core begins with a series of crush zones, which are unsuitable for any direct structural observations (see Figure 5-3). BIPS images, however, allow for the identification of a series of very consistent, gently E/ESE-dipping fractures in the corresponding depth intervals of the borehole. Figure 5-3 shows the crush zone extending from 492.179 down to 492.6 m depth and the average orientation of some of its fractures.

Between c. 494 and 498 m depth there occurs a complex structural pattern, whereby a steep brittle/ductile shear zone, characterised by a pervasive foliated interval in which foliation planes are defined by epidote layers and red stained feldspar and plagioclase (Figure 5-4a and b), is overprinted by a major cataclastic core (Figure 5-4c, d and e). The latter contains cataclasites, ultracataclasites and pockets/layers of green gouge (Figure 5-4d). Brittle deformation postdates the ductile fabric as shown by the fact that the cataclastic rocks formed at the expense of the ductilely foliated granitoids. As illustrated by the black great circles of the stereonet in Figure 5-4, foliation planes dip rather steeply to the SSE, but unfortunately no kinematic indicators were observed in connection with this ductile fabric. The orientation of fractures within the cataclastic core (as derived from the BIPS images) is plotted by the red great circles. These have a very similar orientation to the ductile fabric, which in turn suggests a control of the early ductile structures on the later brittle features.

Figure 5-4e, an extract from the BIPS image, shows the borehole section that corresponds to the cataclastic/ultracataclastic core, within which there also occur core loss intervals due to the low cohesion of the mechanically disrupted rocks.

The granitic host rock remains protocataclastic over a rather long length interval, and generally very deformed and fractured. Due to the numerous fractures, crush zones and core loss intervals, it was at times difficult to establish the exact adjusted length of specific structural features.

Sealed epidote networks (associated with minor dilation and cataclasis) are commonly observed down to about 500 m depth (Figure 5-5).

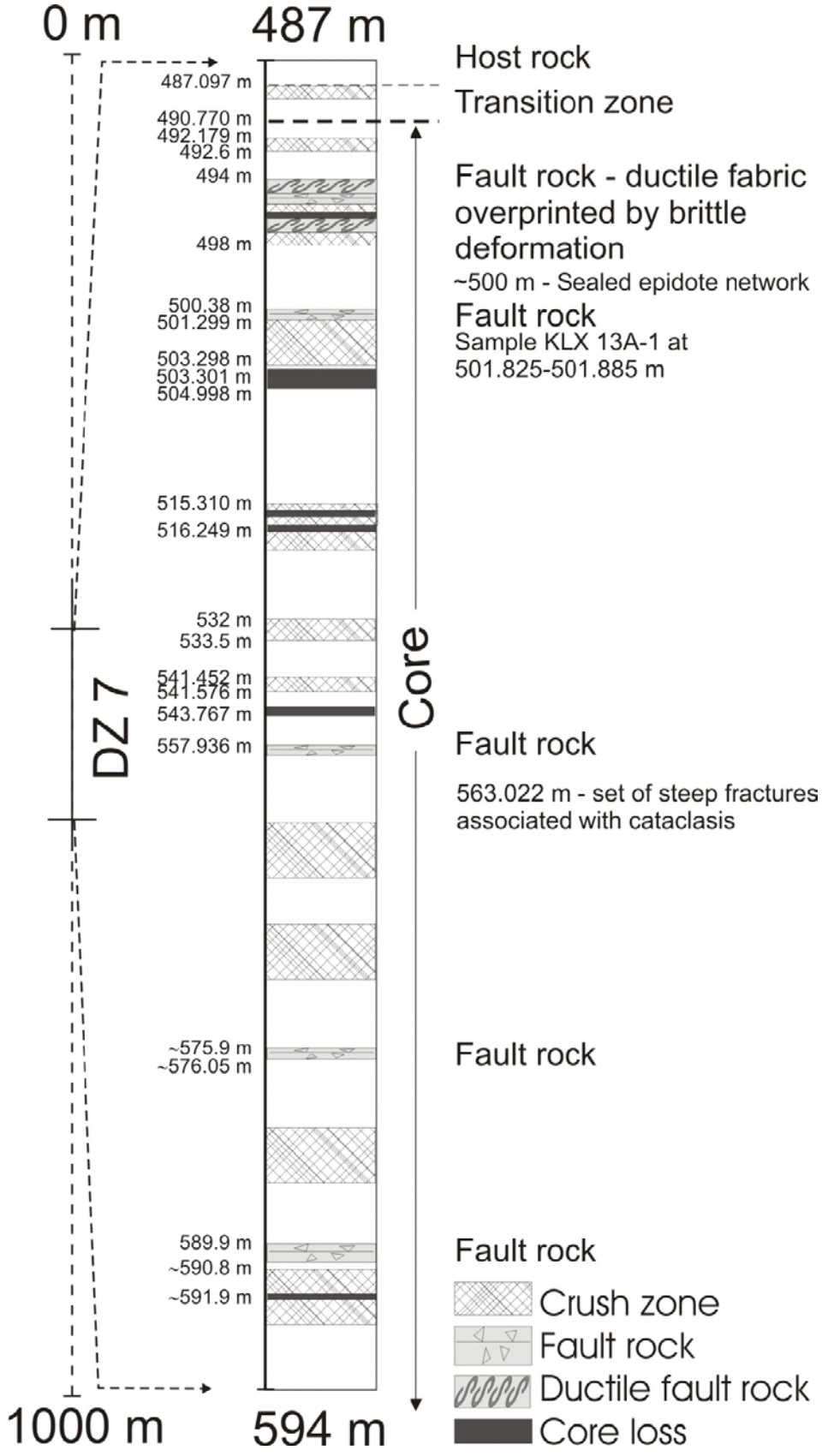

Figure 5-2. *Structural log of DZ 7 in KLX13A. Vertical scale is schematic.*

Figure 5-3. *Look and orientation of the uppermost crush zones within the core of DZ 7.*

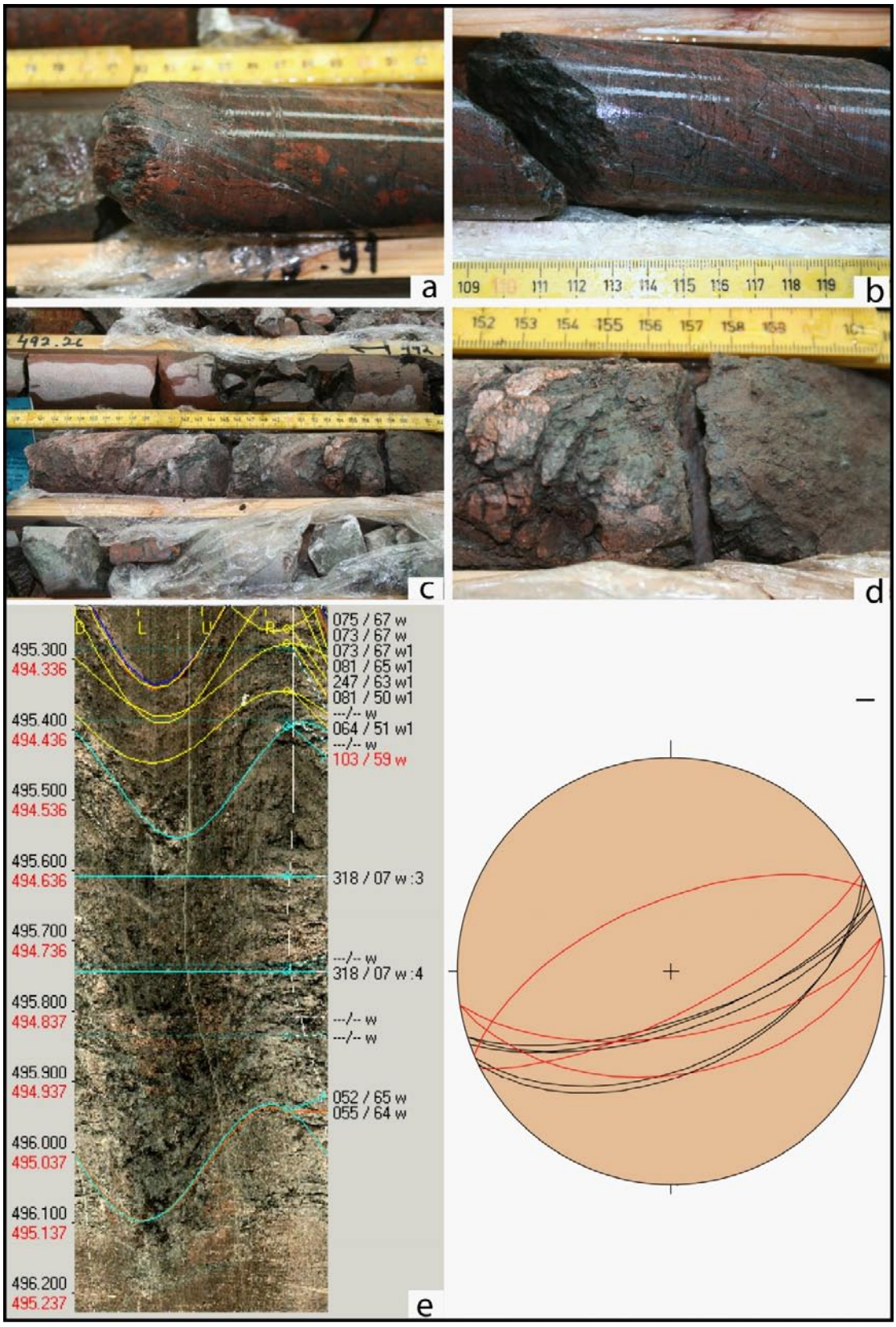

Figure 5-4. *a) and b): Example of pervasive foliation within depth interval 494–498 m. c) and d): Detail of the major cataclastic core that overprints the ductile fabric. Cataclasites formed at the expense of the strongly foliated granitoids. e): BIPS image of the same depth interval, showing the presence of a major cavity in the borehole wall coincident with the cataclastic core. The stereonet plots the orientation of foliation planes (black great circles) and of fractures within the cataclastic core (red great circles, as derived from the BIPS image).*

Figure 5-5. *Sealed epidote network and minor cataclasis observed to about 500 m depth.*

The next significant structural feature is observed within depth interval 500.38–500.60 m, where there occurs a dense network of fine-grained, red/brown ultracataclasite and gouge bands, associated with a few hematite-chlorite- and calcite-coated striated surfaces. The dominant bands and fractures dip moderately to the NE and the kinematics established for one striated plane suggest sinistral strike-slip shear (Figure 5-6).

At depth 501.299 we locate the upper limit of a long crush zone that extends to depth 503.298 m. Fractures in it dip moderately to the ESE and SE (Figure 5-7).

A significant core loss, probably due to the presence of a strongly fractured rock interval, is found within depth interval 503.301–504.998 m. The orientation of a few fractures within this zone could be derived from the oriented borehole image (Figure 5-8).

Although a couple of fracture planes strike NE-SW, most measurements indicate a c. NW-SE trend for the fractures within this zone of core loss. No kinematic indicators were observed.

The core does not contain any particularly interesting structural feature down to c. 515 m, apart from a few striated fault planes (Figure 5-9). These are coated invariably by chlorite and calcite, and locally clay minerals and hematite. A rather heterogeneous kinematic picture emerges from their stereographic projection, with very different orientations and kinematics (Figure 5-9).

Figure 5-10a shows the apparently poorly deformed rock interval in the borehole at depth 515.310 m. This depth interval, however, corresponds to the upper part of a c. 40 cm thick crush zone. Figure 5-10b plots the orientation of several fractures from yet another long crush zone that starts at depth 516.249 m. Apart from a few very steep NNW-SSE trending fractures, the remaining fractures dip gently to moderately to either the NNE, NE or WSW.

A particularly strongly fractured interval is found at depth 532 m and extends down to c. 533.5. Figure 5-11 plots the orientation of a few fractures from this depth interval: mostly NS striking and moderately E-dipping open fractures were observed.

Figure 5-6. *Dense network of fine-grained, red/brown ultracataclasite and gouge bands, associated with a few hematite-chlorite- and calcite-coated striated surfaces at depth 500.38 m and relative orientation.*

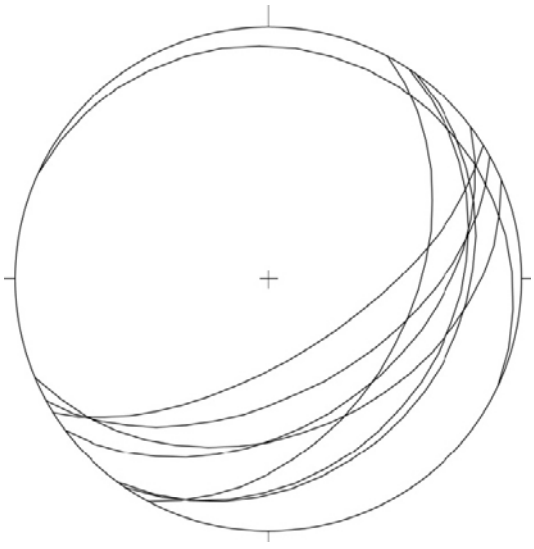

Figure 5-7. *Fracture orientation within the crush zone extending from 501.299 down to 503.298 m depth.*

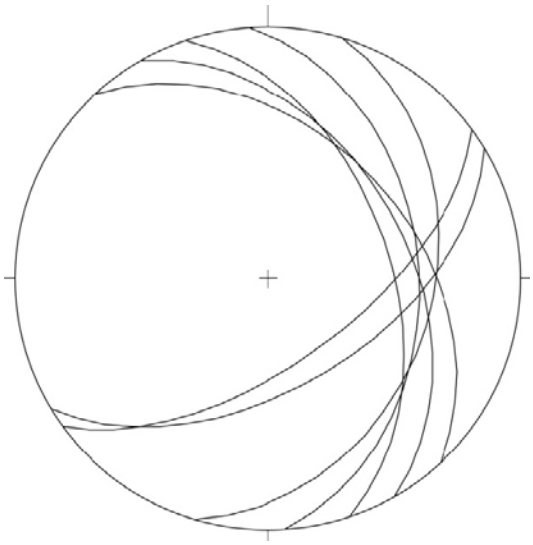

Figure 5-8. *Fracture orientation (derived from BIPS images) within depth interval 503.301 and 504.998 m.*

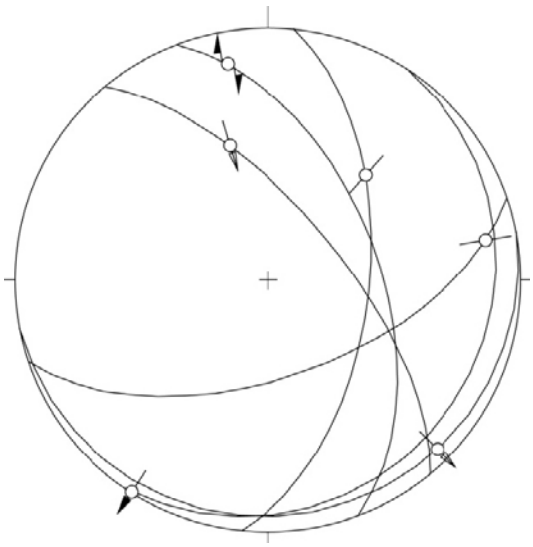

Figure 5-9. *Orientation and kinematics of striated surfaces within depth interval 508–515 m.*

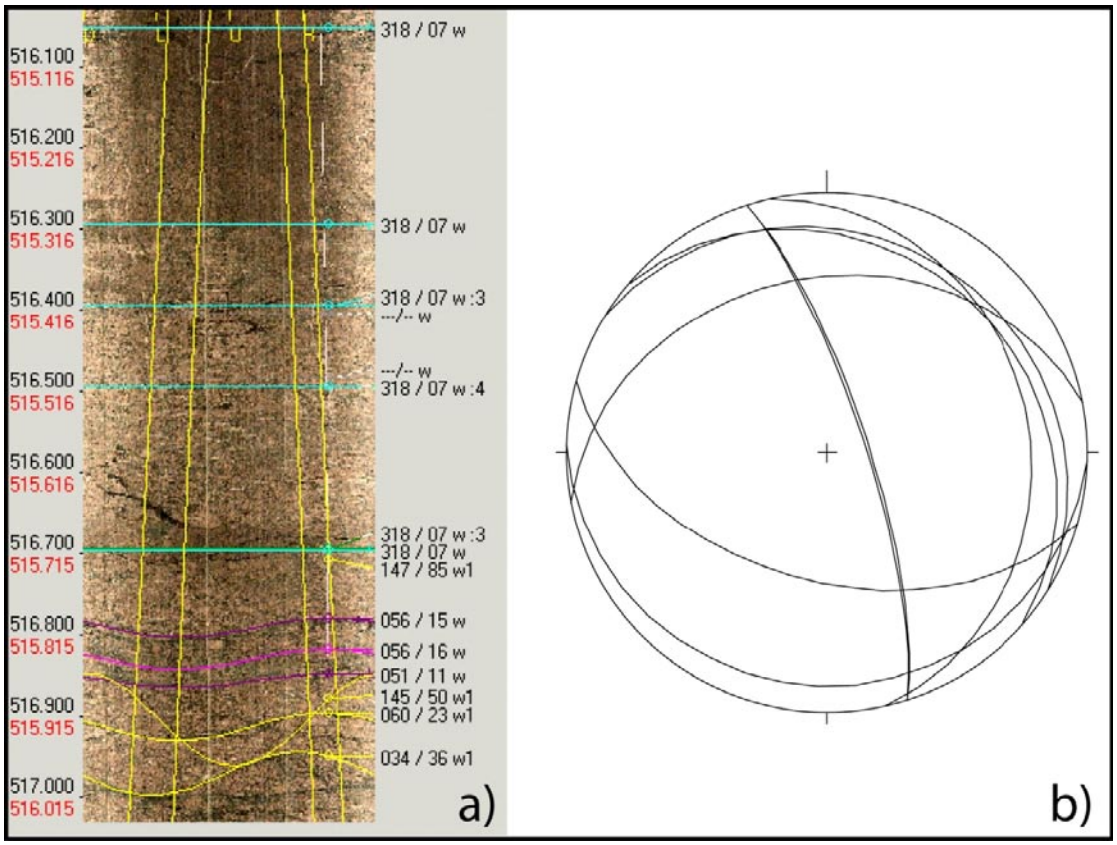

Figure 5-10. *a) BIPS image of an apparently weakly deformed depth interval, which nonetheless corresponds to a c. 40 cm thick crush zone in the recovered core. b) Fracture orientation in another crush zone starting from depth 516.249 m.*

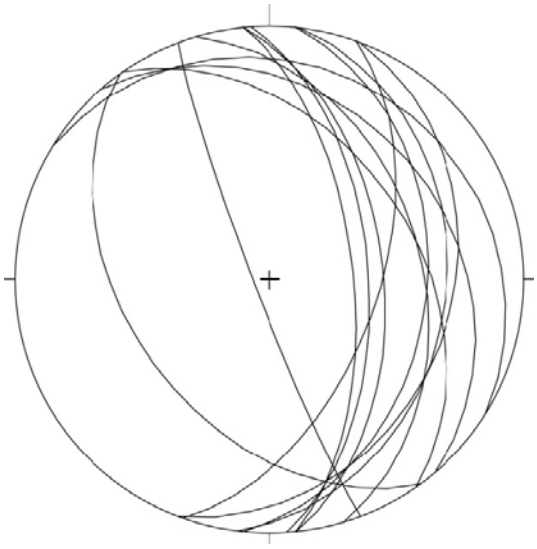

Figure 5-11. *Fracture orientation within an intensively fractured depth interval from 532 down to 533 m depth.*

Several other thin crush zones are found, but are interpreted here as only minor features. A strongly fractured interval extends from 541.452 to 541.576 m depth and is followed by another severely fractured interval passing laterally to a zone of core loss from 543.767 m to 543.967 m depth. Fractures from these two intervals can be grouped into three different systematic sets (Figure 5-12), with conjugate fractures striking WNW-ESE, NE-SW and NNW-SSE. Whereas the first two sets have gentle to moderate dips, the last is characterised by very steep, subvertical dip angles.

A c. 30 cm thick cataclastic core is found at depth 557.936 m. The core contains dilational calcite veins that postdate, intruding into and disrupting, earlier brittle fabrics also containing veins of brown ultracataclasites/gouge. A single fracture plane was measured and it is oriented EW, with a moderate dip to the S (Figure 5-13).

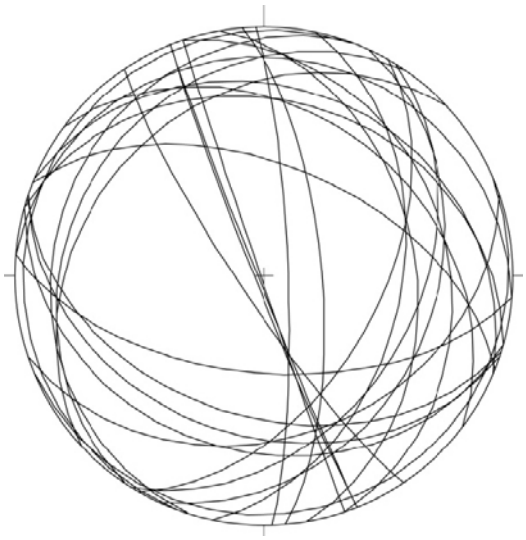

Figure 5-12. *Fracture orientations for depth interval 541.452–541-576 m and the fractured interval preceding the core loss zone starting at 543.767 m.*

Figure 5-13. *EW-trending and moderately S-dipping cataclastic core at depth 557.936 m. Note the late dilational calcite veins disrupting earlier cataclastic fabrics.*

The remaining core section contains several striated surfaces, coated by chlorite, calcite and locally hematite and clay minerals (Figure 5-14).

At depth 563.022 there occurs a set of steep fractures, locally associated with cataclastic bands and grain size reduction of the granitic host rock (Figure 5-15).

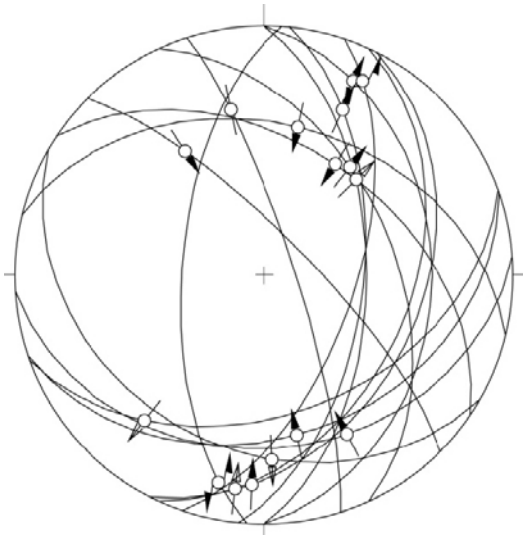

Figure 5-14. *Orientation and kinematics of striated fracture planes from the bottom part of DZ 7.*

Figure 5-15. *Steep fractures at depth 563.022, locally associated with cataclasis of the granitic host rock. The fractures strike NS to NNW-SSE and dip very steeply to the E, ENE.*

Table 5-1. Summary of DZ 7.

Depth (m)	Box number	Interpretation	Description
486	72	Host rock	Undeformed rock.
487.097–490.770	72	Transition	Increase in fracture frequency and red staining.
490.770– (594)	72–92	Core	
490.770–~491.30	72		Crush zone.
~491.30– ~491.71	72		Fractured rock.
~491.71–~491.80	73		Crush zone.
~491.80– ~493.25	73		Undeformed interval.
~493.25–494.266	73		Pervasive ductile fabric.
494.266–495.053	73		Breccia.
495.053–~495.84	73		Core loss and crush zone.
~495.84– ~496.35	73		Ductile fabric.
~496.35– ~496.55	73		Crush zone.
~496.55– ~496.75	73		Fractured interval.
~497.27– ~498	74		Crush zone and core loss.
~498– ~498.3	74		Fractured rock.
~498.3– ~498.4	74		Crush zone.
~498.4– ~499.3	74		Fractured rock interval.
~499.3– ~499.4	74		Crush zone.
~499.4– ~500.38	74		Fractured rock interval.
~500.38– ~501.4	74		Undeformed rock.
~501.4– ~~501.5	74		Crush zone.
~501.5– ~501.7	74		Fractured rock.
~501.7– ~502.65	74–75		Crush zone, containing gouge bands and epidote sealed networks.
~502.65– ~503.65	75		Crush zone.
~503.301–~504.998	75		Core loss.
~504.80–~507.05	75		Fractured rock.
~507.05– ~511.41	75–76		Undeformed rock, with some epidote networks and veins.
~511.41– ~512.4	76		Highly fractured rock interval.
~512.4– ~512.6	77		Crush zone.
~512.6– ~513.6	77		Fractured rock.
~513.6– ~513.7	77		Crush zone.
~513.7– ~513.8	77		Epidote network.
~513.8– ~513.9	77		Crush zone.
~513.9– ~514.75	77		Fractured rock with epidote networks.
~514.75– ~514.9	77		Crush zone.
~514.9– ~515	77		Core loss interval.
~515– 515.3	77		Fractured rock.
~515.3– ~515.5	77		Crush zone.
~515.5– ~515.6	77		Core loss interval.
~515.6– 516.249	77		Fractured rock interval, with fractures subparallel to the axis of the core and later shallower dipping fractures.
516.249– ~516.65	77–78		Crush zone.
~516.65– ~518.08	78		Fractured rock with epidote networks.
~518.08– ~518.28	78		Crush zone.
~518.28– ~518.99	78		Fractured rock interval.
~518.99– ~519.3	78		Crush zone.
~519.3– ~519.9	78		Fractured rock with calcite veins.
~519.9– 520.543	78		Crush zone.

520.543– 520.932	78	Core loss. Image from BIPS.
520.932– ~521.3	78	Fractured rock interval.
~521.3– ~521.6	78	Crush zone.
~521.6– ~523.14	78–79	Fractured rock interval with a few thin bands of cataclasite (~1–2 cm) and a 0.5 cm band of ultracataclasite and gouge in addition to calcite veins.
~523.14– 523.248	79	Crush zone.
523.248– 523.542	79	Core loss (006/41, 009/42). Possible cataclastic protolith.
523.542– ~524.53	79	Crush zone.
~524.53– ~525.57	79–80	Fractured rock interval.
~525.57– ~527.5	80	Undeformed rock.
~527.5 –~528.5	80	Fractured rock interval.
~528.5– ~531.3	80	Undeformed rock.
~531.3– ~533.35	80–81	Fractured rock with fractures subparallel to the axis of the core and later shallower dipping fractures.
~533.35– ~533.45	81	Crush zone developed at the expense of sealed epidote networks.
~533.44– ~534.26	81	Fractured rock
~534.26– ~535.44	81	Undeformed rock.
~535.44– ~536.5	81	Fractured rock interval.
~536.5– ~536.6	81	Crush zone.
~536.6– ~541.27	81–82	Fractured rock with a thin band, ~2 cm thick, of cataclasite, plus epidote networks.
~541.27–~541.4	82	Crush zone.
~541.4–~541.5	82	Core loss interval.
~541.5– ~543.7	82–83	Fractured rock interval.
~543.7– ~543.7	83	Core loss interval.
~543.7– ~547.3	83	Fractured rock with a 1–2 cm thick band of gouge and some epidote veins.
~547.3– ~547.4	83	Crush zone.
~547.4– ~548.2	83	Fractured rock interval.
~548.2– ~548.3	83	Crush zone.
~548.3– ~548.7	83–84	Fractured rock interval.
~548.7–~548.8	84	Crush zone.
~548.8–~548.9	84	Fractured rock interval.
~548.9– ~550.59	84	Undeformed rock.
~550.59– ~550.85	84	Fractured rock interval.
~550.85– ~550.9	84	Crush zone.
~550.9– ~551.62	84	Fractured rock interval.
~551.62– ~551.7	84	Crush zone.
~551.7– ~552.62	84	Fractured rock interval.
~552.62– ~554.59	84–85	Undeformed rock.
~554.59–~554.75	85	Fractured rock interval.
~554.75– ~554.85	85	Crush zone.
~554.85– ~555.25	85	Fractured rock interval.
~555.25–~555.35	85	Crush zone.
~555.35– 557.964	85	Fractured rock interval.
557.964– 558.204	85	Fault rock- red and green gouge, 0.5 cm thick plus cataclasite and ultracataclasite with calcite.
558.204– ~558.54	85	Fractured rock interval along sealed epidote network.

~558.54– ~561.67	86	Undeformed rock interval, with pervasive calcite veining.
~561.67– ~563.5	86	Fractured rock interval containing epidote networks and later calcite veins. Possible cataclastic band infilled by chlorite and calcite at ~563.260 m
~563.5– ~564.79	87	Undeformed rock.
~564.79– ~568.2	87	Fractured rock, thin, 0.5 cm thick fracture filling with red gouge.
~568.2– ~568.35	87	Crush zone.
~568.35– ~571.05	87–88	Fractured rock interval.
~571.05– ~571.10	88	Crush zone.
~571.1– ~572.2	88	Fractured rock with epidotization and veins.
~572.2–~572.3	88	Crush zone.
~572.3– ~574.2	88–89	Fractured rock interval.
~574.2–~574.3	89	Crush zone.
~574.3–~575.4	89	Fractured rock, 5–7 cm thick epidote vein.
~575.4–~575.45	89	Crush zone.
~575.45–~575.9	89	Fractured rock interval.
~575.9– ~576.05	89	Fault rock, 10–12 cm thick, consisting of protocataclasites and dilatant epidote networks.
~576.05–~576.3	89	Fractured rock interval.
~576.3– ~576.5	89	Crush zone.
~576.5– ~578.4	89–90	Fractured rock interval.
~578.4–~578.75	90	Crush zone.
~578.75– ~585.6	90–91	Fractured rock interval.
~585.6– ~585.75	91	Crush zone.
~585.75–~586.15	91	Densely fractured rock.
~586.15–~586.5	91	Crush zone.
~586.5– ~588.9	91–92	Undeformed rock.
~588.9–~589.25	92	Crush zone.
~589.25–~589.45	92	Undeformed rock.
~589.45– 589.90	92	Fractured rock interval.
589.90– 590.10	92	20–25 cm thick cataclasite- ultracataclasite and gouge interval.
590.10– ~590.70	92	Fractured rock interval.
~590.70–~590.85	92	Cataclasite band and epidote sealed network.
~590.85– ~591.05	92	Fractured rock interval.
~591.05–~591.10	92	Crush zone.
~591.10– ~591.75	92	Fractured rock interval.
~591.75– ~591.9	92	Crush zone.
~591.9–~592.05	92	Core loss interval.
~592.05– ~592.2	92	Crush zone.
~592.2– ~593.64	92	Densely fractured rock.
		End of core

5.2 KLX15A

The location of KLX15A is shown in Figure 5-1. The core is 1,000.43 m long, is oriented 193/48 and penetrates in Ävrö granites /Carlsten et al. 2008a/. The interval logged during this study extends from 706 to 747 and from 978 to 1,000 m depth and includes two separate deformation zones, DZ 16 and 20, respectively.

5.2.1 DZ 16: depth interval 706–744 m

DZ 16 covers a depth interval of c. 40 m and extends from depth 706 to depth 747 m (Figure 5-16). The main rock type logged in it is a medium-grained, homogeneous quartzmonzonite, locally intruded by coarse-grained pegmatites. Red staining is diffuse and is invariably associated with localised shearing and brittle faulting. In general, DZ 16 contains little pervasive deformational features and in our opinion it does not fulfill the structural requirements to be classified as a proper deformation zone. In fact, long sections of it are made of by basically undeformed quartzmonzonites without any evidence of significant structural overprinting.

Nonetheless, the detailed analysis and logging of the section suggests the presence of four distinct fault cores at different depth within DZ 16. These are generally very minor in terms of size and significance and never exceed 50 cm of thickness.

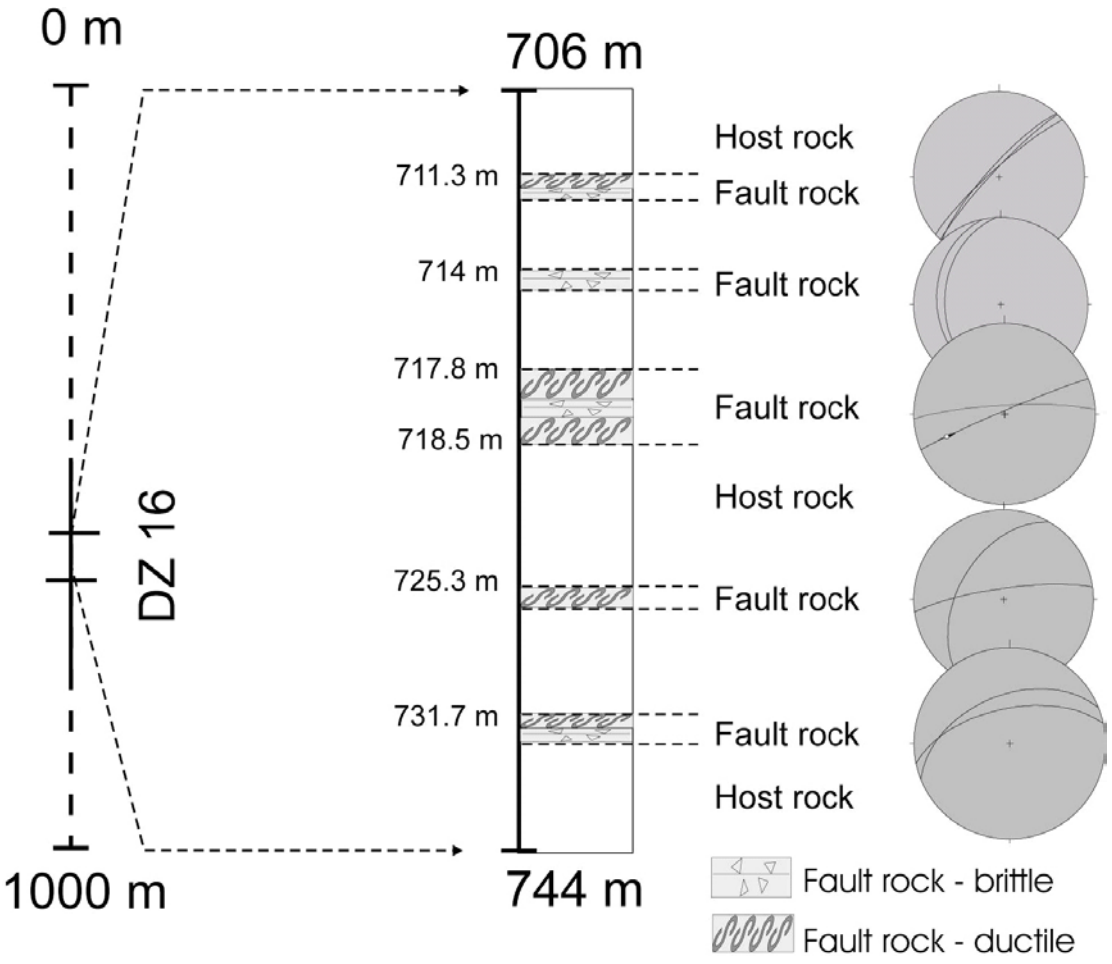

Figure 5-16. *Structural log of DZ 16 in KLX15A. Stereonets are discussed in detail in the text. Vertical scale is schematic.*

The first interesting structural feature, a c. 25 cm thick ductile foliated sequence, occurs at depth 711.379 m. Its upper limit coincides with the lower contact of a thin pegmatite that intrudes into undeformed quartzmonzonites (Figure 5-17). The pervasive foliation dips subvertically to the NW (Figure 5-17). At the lower end of the foliated interval there occurs a c. 4 cm thick cataclastic band. The deformation core ends at depth 711.535, and is not followed by a well-defined transition zone.

A second, distinct thin core is found at depth 714.09 m, where a series of subparallel broken fractures, oriented c. NS and dipping moderately to the W, define the upper limit of a c. 15 cm thick fault rock sequence containing several strands of ultracataclasite/gouge (Figure 5-18). Abundant pyrite is found coating the broken fracture surfaces.

Another minor DZ core starts at depth 717.855 m and is characterised by pervasively foliated quartzmonzonites oriented 267/82 (Figure 5-19). At the upper contact of the foliated interval, quartzmonzonites are intruded by a pegmatite, which is in turn reworked cataclastically (Figure 5-19). Late calcite veins crosscut the contact and their associated dilation creates small pockets of coarse calcite-cemented breccias (Figure 5-19). A striated plane in the middle of the foliated interval shows dextral transpressive shearing along a subvertical ENE-WSW-striking plane (black great circle in Figure 5-19). No obvious and characteristic transition zones are observed above or below this narrow DZ core.

At depth 725.344 m there is a set of two epidote-decorated brittle-ductile shear zones, one relatively steep and the other subvertical. The latter is oriented 262/80, thus not dissimilar from the orientation of the foliation of the ductile core at depth 718 m, whereas the former runs 210/48. Unfortunately no clear crosscutting evidence could be observed.

A last DZ core is observed at depth 731.770 m and extends down to 732.152 m. It is defined by a pervasively foliated interval, with foliation planes dipping moderately to the NNW (Figure 5-21).

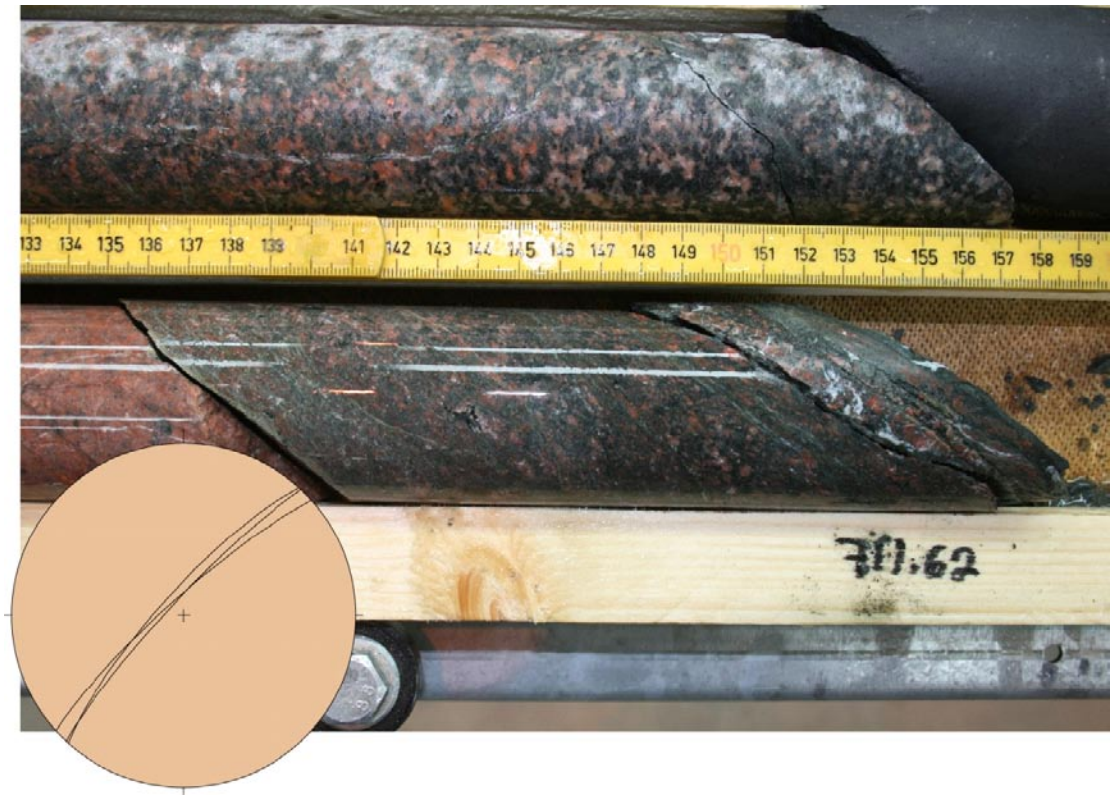

Figure 5-17. *Pervasively foliated sequence at depth 711.379 m. Foliation planes strike NE-SW and dip subvertically to the NW. A c. 4 cm thick cataclastic band marks the lower termination of the foliated sequence.*

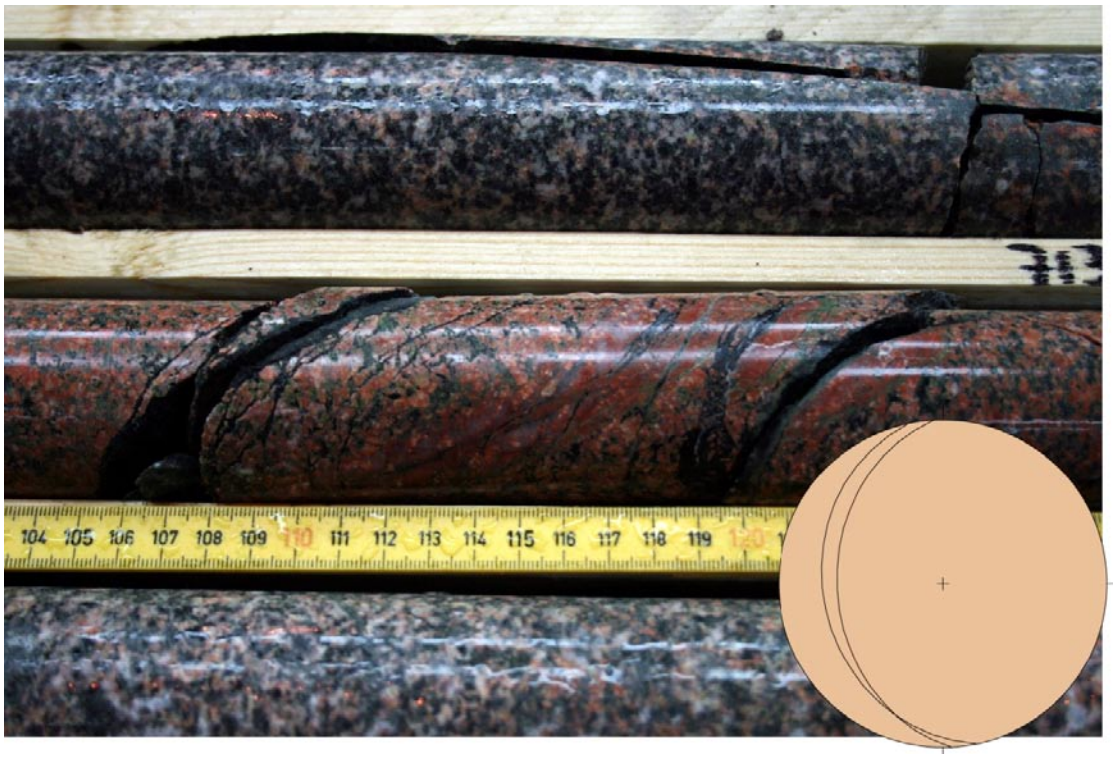

Figure 5-18. *NS striking and W dipping fractures and cataclasite/gouge bands at depth 714 m.*

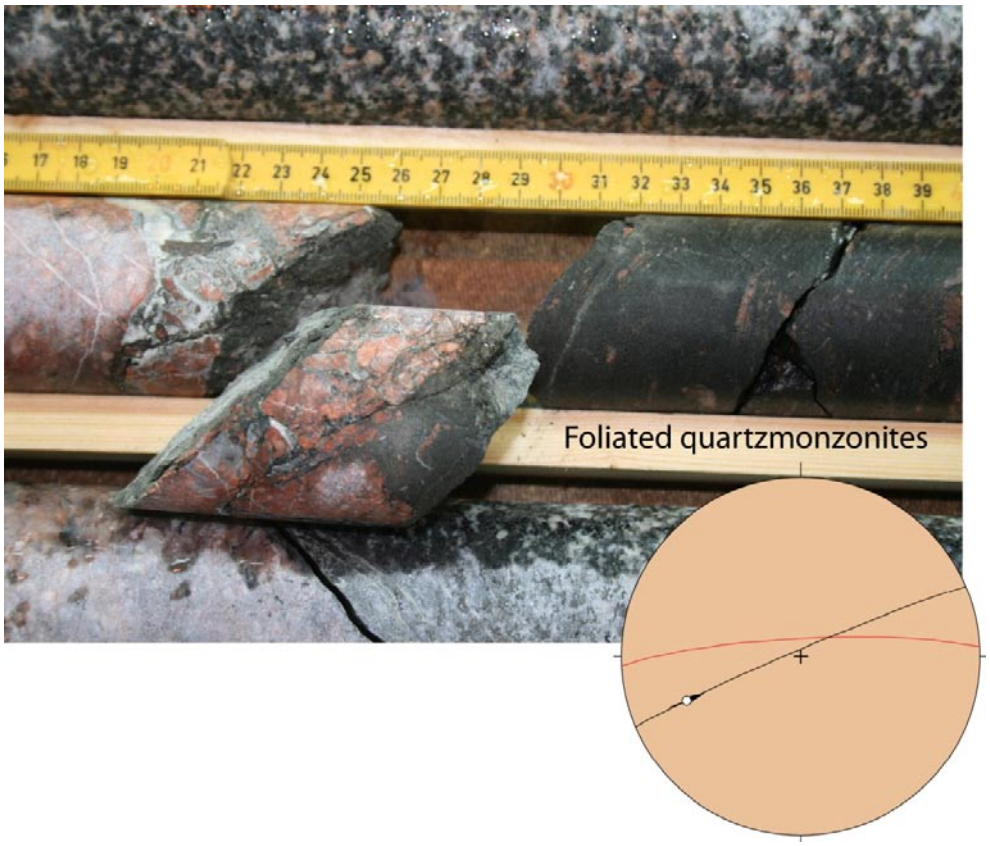

Figure 5-19. *Pervasively foliated quartzmonzonites at depth 717.8 m dip subvertically to the N (average orientation shown by red great circle). Their upper contact to a thin pegmatitic intrusion is disrupted by cataclasis and dilatant calcite veins. The dextral kinematics shown by the black great circle and its associated striation were measured in the middle of the foliated interval.*

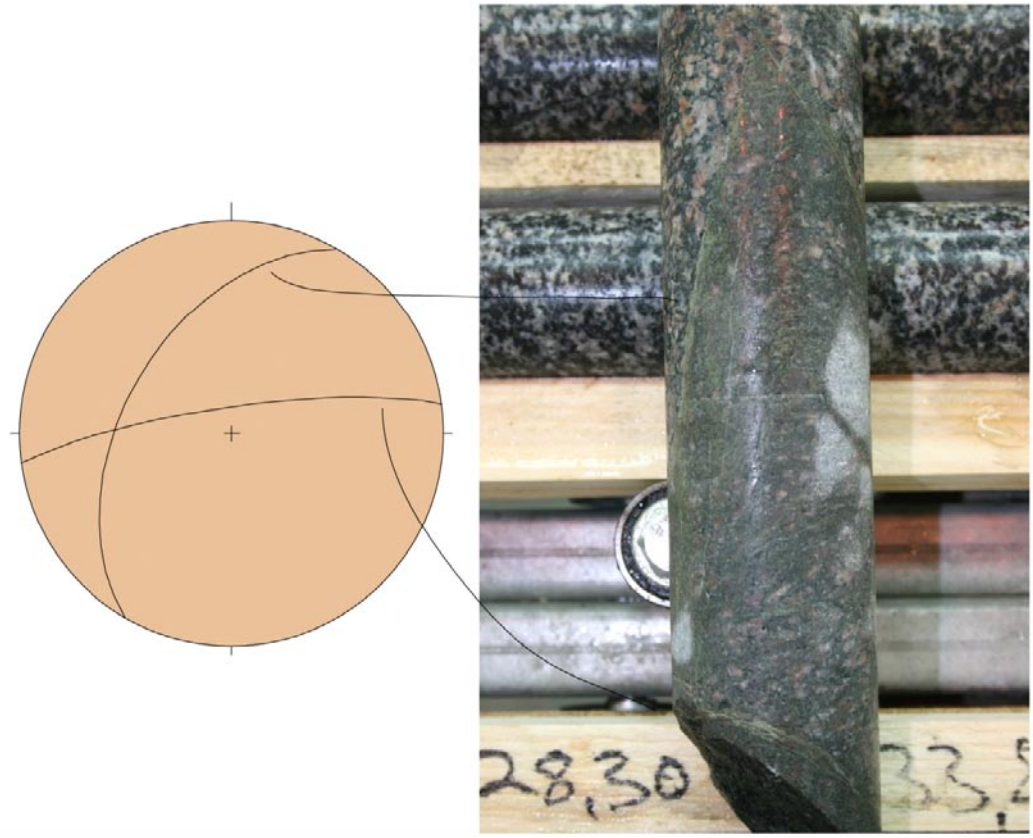

Figure 5-20. *Set of two narrow epidote shear zones found at depth 725.344 m.*

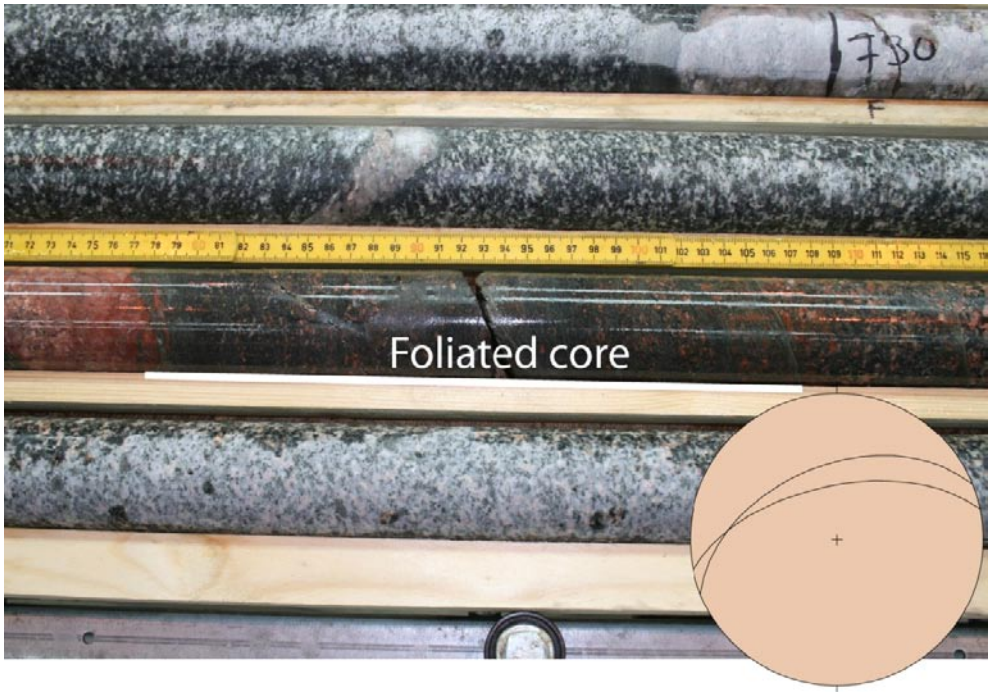

Figure 5-21. *Foliated core extending from depth 731.7710 m down to 732.152 m. Foliation planes strike WSW-ENE and dip moderately to the NNW.*

Throughout the logged interval, but particularly below depth 730 m, several striated planes were observed, measured and constrained kinematically. The results of our observations are shown in Figure 5-22.

Although no clear kinematic pattern emerges, it is noteworthy that most of the striated surfaces show strike-slip kinematics with a general lack of down-dip displacement vectors.

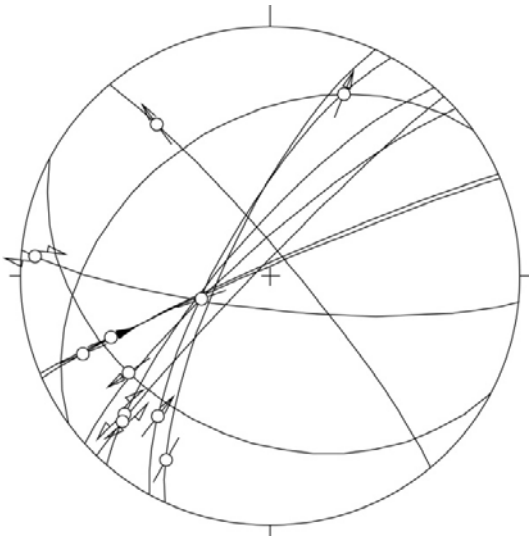

Figure 5-22. *Fault-slip data for DZ 16, mostly observed below depth 730 m.*

Table 5-2. Summary of DZ 16.

Depth (m)	Box number	Interpretation	Description
706–	116	Host rock	Quartz monzonite. Undeformed rock with a few, thin cataclastic bands epidote veins networks.
711.379–711.535	116–117	Core	Ductile fabric characterised by a pervasive foliation and minor foliated cataclasites at the bottom of the sequence.
711.535–~711.92	117		Red staining.
~711.92–~713.85	117	Host rock	Undeformed host rock.
~713.85–714.091	117		Red staining.
714.091–714.236	117	Core	Narrow core with cataclasites.
714.236–~714.58	117		Red staining.
~714.58–717.855	117–118	Host rock	Undeformed rock.
717.855–718.55	118	Core	Foliated core overprinted by cataclasites and ultracataclasites, plus possible cemented breccia.
718.55–725.344	118–119	Host rock	Undeformed rock.
725.344–725.509	119	Ductile core	Ductile fabric associated with epidote shear zones.
725.509–731.770	119–120	Host rock	Undeformed host rock with thin pegmatitic dikes, calcite veins and epidote vein sealed networks.
731.770–732.152	120	Brittle-ductile core	Foliated core.
732.152–743	120–122	Host rock	Undeformed rock with epidote vein networks, calcite veins and pegmatite dikes.

5.2.2 DZ 20: depth interval 976–1,000 m

No borehole images are available for this DZ and therefore no structural features could be oriented. DZ 20 is characterised in its upper part by a transition zone extending from c. 978 to 986 m depth (Figure 5-23). This is defined by a progressive increase in fracture frequency, which in the central part of the transition zone reaches values of up to 17 f/m, thus possibly indicative of a DZ core.

A proper core, however, is found starting at ~995 m depth. No information on its termination is provided here because the end of the DZ was not logged due to the termination of the KLX15A drill core. There is a sharp boundary between undeformed host rock and the core, which is defined by an early ductile fabric. This fabric is overprinted by brittle deformation that generated proto-cataclasites and cataclasites, with a very high fracture frequency (up to 50 f/m) forming crush zones and leading to localized core loss.

Table 5-3: Summary of DZ 20.

Depth (m)	Box number	Interpretation	Description
976–978.55	164	Host rock	Undeformed rock.
978.55–986.20	164–165	Transition zone	Higher fracture frequency than the host rock (up to 17 f/m). Diffuse red staining.
986.20–994.70	165–167	Host rock	Undeformed rock, with epidote networks, calcite veins and red staining. Low fracture frequency.
994.70–	167–168	Ductile to brittle core	Sharp boundary between undeformed rock and DZ core. Ductile fabric overprinted by cataclasites. Locally extremely high fracture frequency, up to 50 f/m.

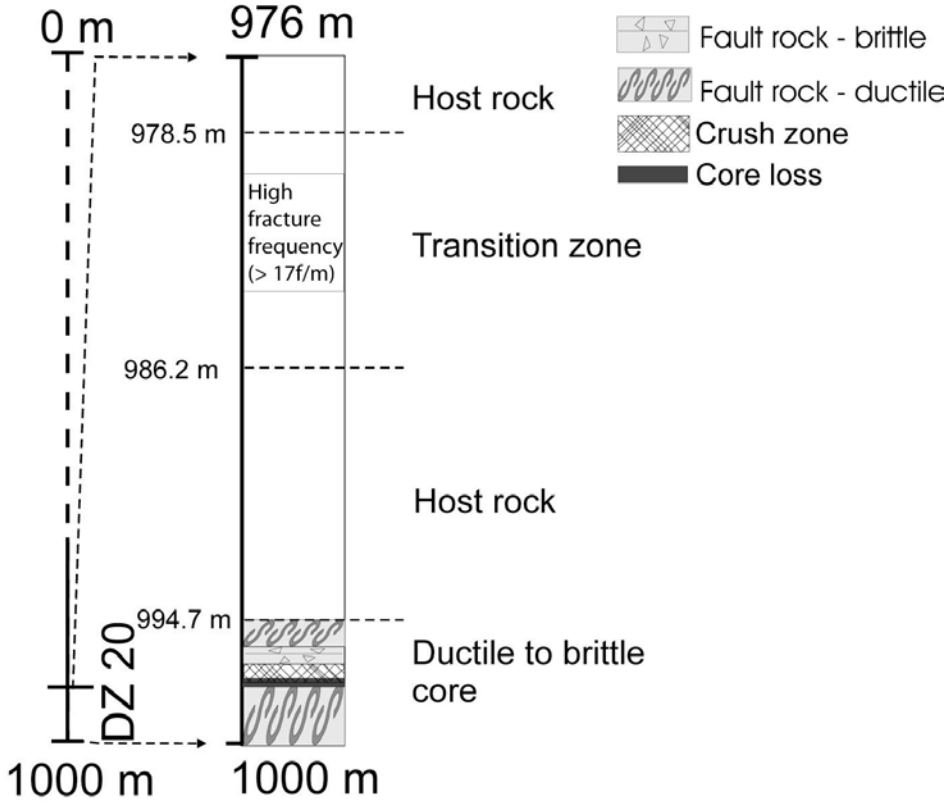

Figure 5-23. *Structural log of DZ 20 in KLX15A. The drill core is oriented 190/47 within this depth interval. Vertical scale is schematic.*

5.3 KLX16A

The location of KLX16A is shown in Figure 5-1. We logged DZ 12 (Figure 5-24), straddling the 325–435 m depth interval. Within this depth interval the drill core is oriented 296/64 and penetrates in quartz monzodiorites /Carlsten et al. 2007b/.

5.3.1 DZ 12: depth interval 325 – 435 m

DZ 12 in KLX16A contains most of its interesting structural features in the upper part. A first, minor low-grade ductile shear zone is found at depth 330.091 m. It is characterised by a subvertical, NW-dipping foliation, defined by epidote (Figure 5-25).

An upper brittle core starts at depth 338.730 m, is c. 20 cm thick and is defined by a cataclastic sequence formed at the expense of quartz monzodiorites. No clear orientation information could be obtained for the core, apart from a single fracture oriented 047/45.

A second cataclastic core starts at 340.908 m depth and continues down to c. 341.75 m (Figure 5-24 and Figure 5-27). It is defined by a spectacular cataclasite-ultracataclasite/cemented breccia. A narrow core loss interval is also associated with this core and the core upper and lower limits could thus be identified only from borehole images. No information about to the orientation of the core is available.

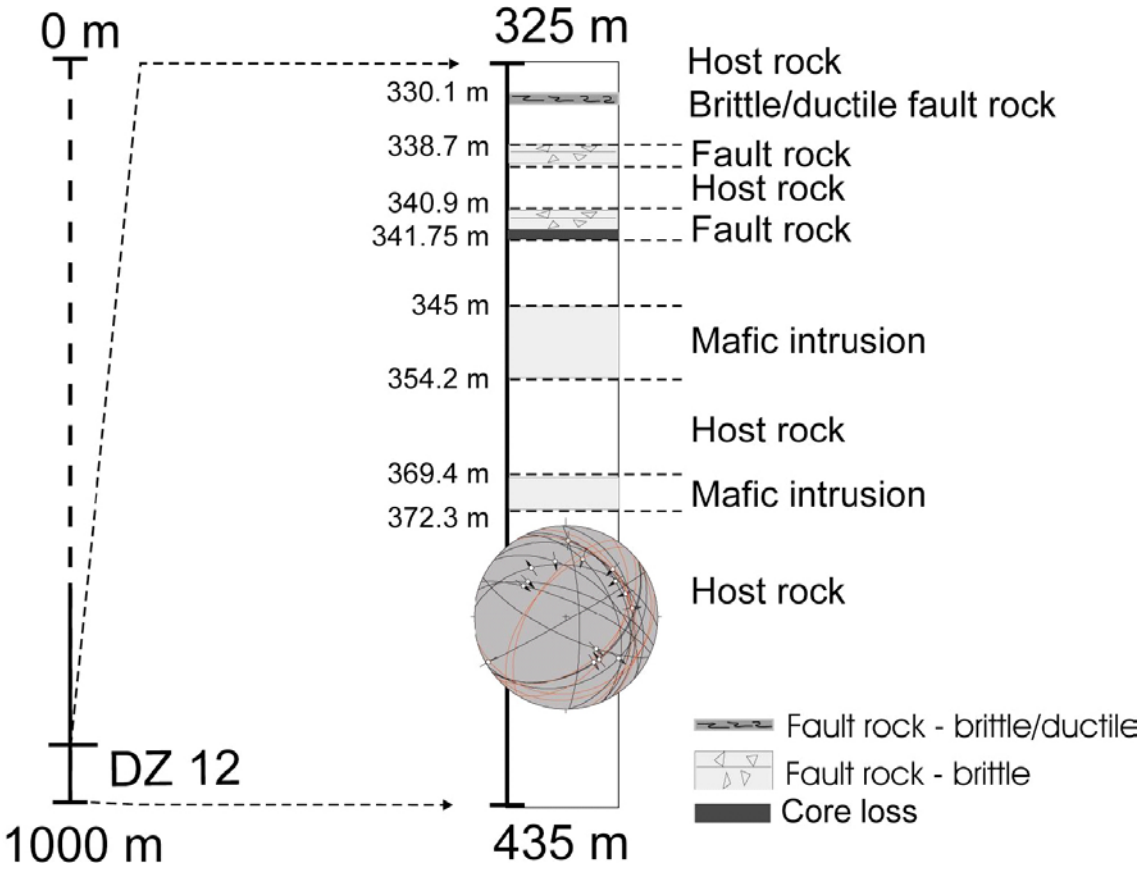

Figure 5-24. *Structural log of DZ 12 in KLX16A. The stereonet shows the orientation of several thin cataclastic bands (red great circles) and slickensided fractures observed in the deepest portion of DZ 12. Vertical scale is schematic. See the text for more details.*

Figure 5-25. *Foliated interval at depth 330.091. Foliation planes, outlined by epidote, dip subvertically to the NW.*

Figure 5-26. *Cataclastic core at depth 338.73 m in KLX16A (below the red line). Note the high fracture frequency and the development of minor crush zones.*

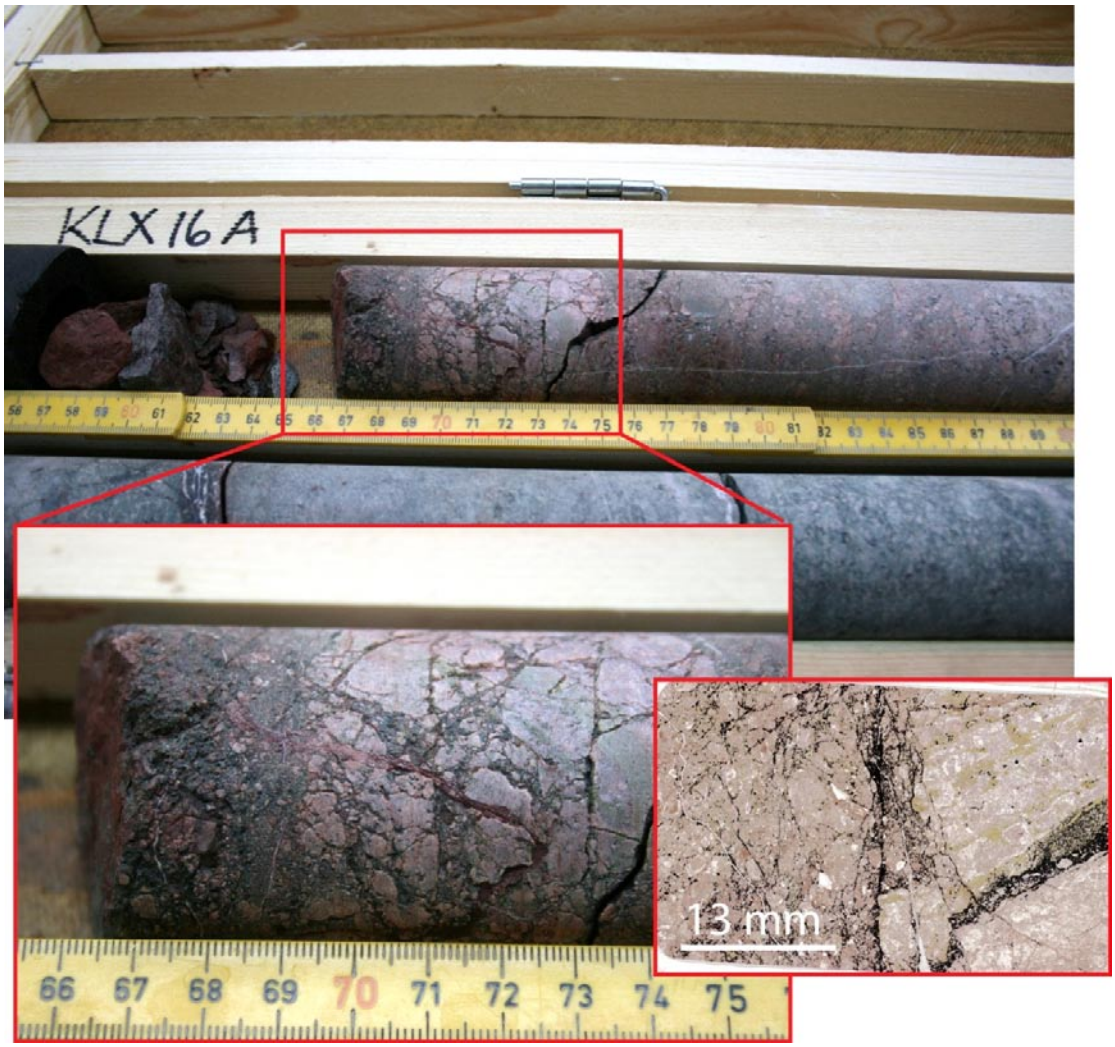

Figure 5-27. *Cataclastic core at depth 340.908. The enlargement shows the details of the angular nature of the poorly sorted clasts within the cataclasite. The scanned thin section of sample KLX16A1 shows several narrow brittle fault branches affecting the undeformed host rock (to the right) and converging into a single broader deformation zone, which is transitional to the cataclastic component of the DZ core (to the left hand side).*

At depth 356.654 m there is a discrete fault plane, oriented 294/68, which offsets with reverse kinematics two subparallel and extremely thin ultracataclastic bands (Figure 5-28).

There are several other cataclastic bands in the core, but they are extremely thin and not associated with significant deformation. Their orientation is shown by the red great circles in the stereonet of Figure 5-29. They dip moderately to the SE, NE and NW.

The lower part of the DZ contains several striated fractures that were constrained kinematically. Figure 5-29 plots them together with the orientation of the thin cataclastic bands. Except for a few high-obliquity shear fractures, most of the slickensided planes constrain dip slip kinematics, predominantly reverse.

Figure 5-28. *Thin discrete NE-dipping fault offsetting two parallel ultracataclastic veins.*

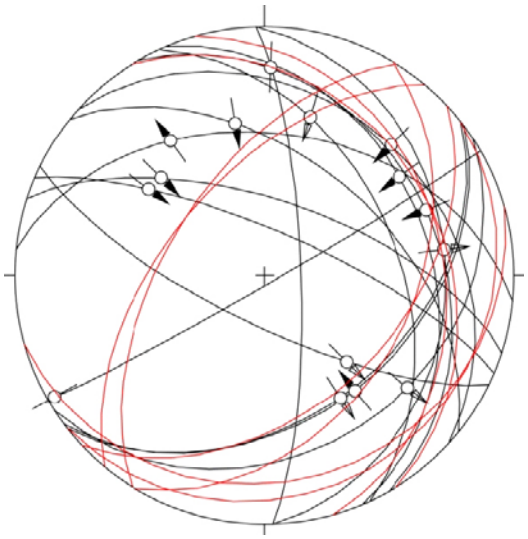

Figure 5-29. *Orientation of thin cataclastic bands (red great circles) and fault slip data for striated planes in the lower part of DZ 12.*

Table 5-4. Summary of DZ 12.

Depth (m)	Box number	Interpretation	Description
325	62	Host rock	Undeformed monzodiorite. Red staining increases with depth, especially from 330.577 m. 330.091–330.577 m corresponds to a brittle-ductile shear zone. Pegmatite dikes are common.
338.73–338.93	64	core	Narrow cataclastic core, 20–25 cm thick.
338.93–~339.25	64		Red staining.
339.25–340.908	64	Host rock	The “zone” begins with a lithological change from monzodiorite to fine grained mafic, intrusive, rock (diabase). Increase in fracture frequency with depth.
340.908–341.10	65	core	Narrow cataclastic core, 8~20 cm thick. Core loss – upper and lower limits of core are taken from BIPS images.
341.10–~341.75	65		Red staining.
~341.75–	65	Host rock	Alternating granite/monzodiorite and fine grained mafic rock with grey or pink colour. Localised epidote networks and veining.
353.332–354.274	67		At depth 353.332 to 354.274 m foliated and banded host rock. The foliation is invariably associated with pegmatitic intrusion.
354.274–369.80	68	Granitic host rock	Diffuse red staining occurs, commonly in association with pegmatite.
~369.80–	70–82	Host rock	Undeformed rock with some thin bands of cataclasite, networks of ultracataclasite and gouge, and veins of calcite, epidote and phrenite. Maximum width of bands is 7 cm. Red staining around pegmatite dykes.

5.4 KLX17A

KLX17A is located in the easternmost part of the Laxemar investigation area, close to the surface lithological boundary between quartz monzodiorites and Ävrö granites (Figure 5-1). Two deformation zones (DZ 1 and DZ 3, covering the depth intervals 98–114 m and 191–228 m, respectively) /Carlsten et al. 2007c/ were logged during this study.

5.4.1 DZ 1: depth interval 98–114 m

DZ 1 is primarily characterised by a c. 3 m thick core that extends from 108.7 m depth down to 111.4 m (Figure 5-30). Due to significant sampling of the core prior to our logging phase in June 2007 and to the numerous zones of core loss, it is virtually impossible to characterise deformation style, geometry and kinematics of this deformation core (Figure 5-31). Large cavities in the borehole image (Figure 5-30) suggest the core to be a zone of extreme mechanical weakness and did not allow the orientation of planare features in the core.

In order to gain insights into possible fracture orientation trends in the core and its proximity, we have measured several fracture orientations in its upper and lower transition zones. These are defined based on increasing and decreasing fracture frequency towards and away from the core, respectively. The stereonets in Figure 5-30 show a slightly different picture for the two zones, with the upper being characterised by typically lower dip fractures and variable dip directions to the E, S, W and all intermediate directions, whereas the lower transition zone contains generally steeper fractures that dip almost unimodally to the SW.

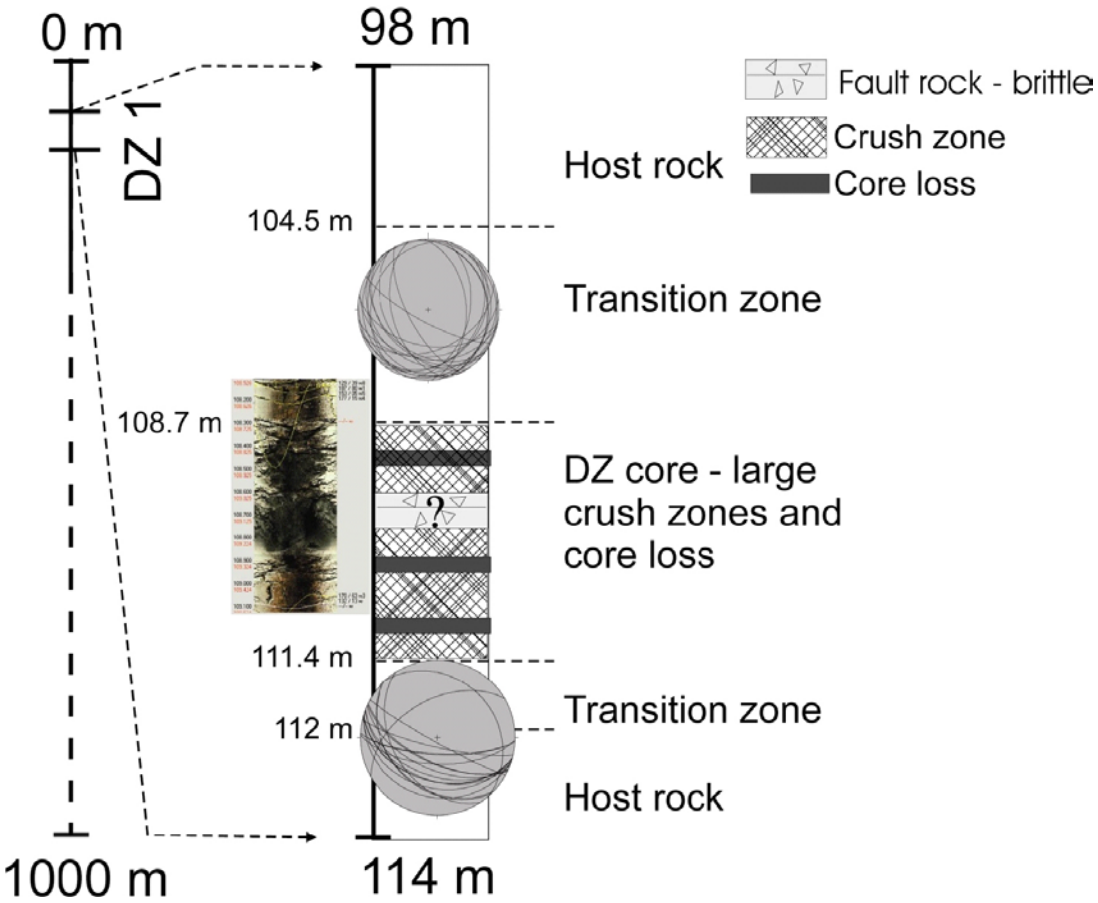

Figure 5-30. *Structural log of DZ 1 of KLX17A. The borehole image shows large cavities in the hole at depths corresponding to the DZ core. Stereonets show the orientation of open fractures (measured from the borehole image) from the upper and lower transition zone. Vertical scale is schematic.*

Figure 5-31. *Due to core loss and sampling, no useful access to the DZ core was possible (depth interval 109–111 m; Box 9).*

Table 5-5. Summary of DZ 1.

Depth (m)	Box number	Interpretation	Description
98	7	Host rock	Occurrence of a minor cataclastic band at 100.226 m (102/44) to 100.293 m (~7 cm), and at 100.401 m (110/43, ~2 cm). Localised red staining.
104.52	8	Transition	Pervasive red staining. Increasing fracture frequency (up to 25 f/m).
108.699	9	Fault core	Significant core loss and crushed zones.
111.40	9	Transition zone	Diffuse red staining. Progressively decreasing fracture frequency.
~112	9	Host rock	Undeformed rock.

5.4.2 DZ 3: depth interval 191–228 m

DZ 3 is developed in porphyritic granites, quartz monzodiorites and diorites. Its main structural feature is a cataclastic fault core, about 35 cm thick, whose upper boundary is located at depth 199.99 m (Figure 5-32). Red staining is very pervasive. The core was sampled prior to our stay in Oskarshamn in June 2007 and we could therefore not characterise it. The two, upper and lower, core-bounding fractures dip extremely shallowly to the S (Figure 5-32).

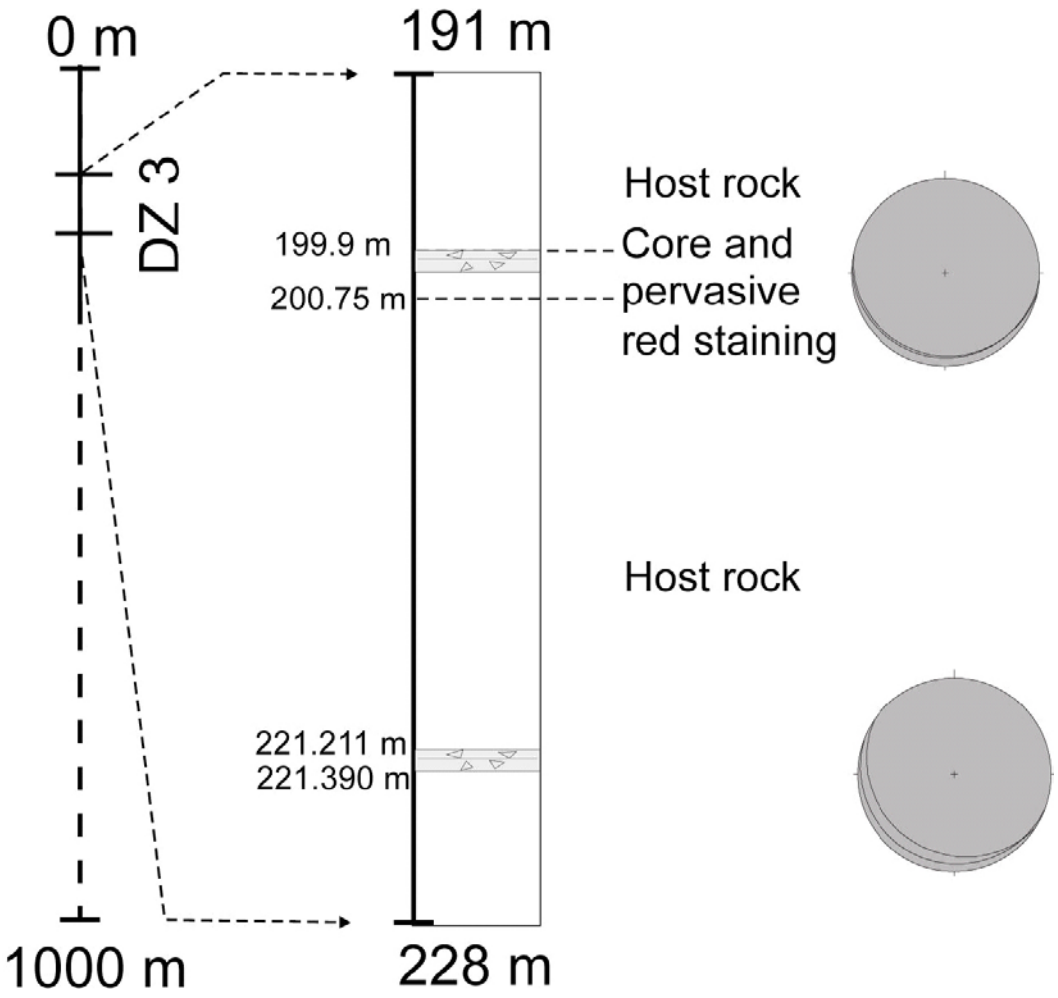

Figure 5-32. *Structural log of DZ 3 in KLX17A. Vertical scale is schematic.*

A second minor core is found at depth 221.211 m. The core, c. 20 cm thick, is characterised by a dense sealed network of fine-grained epidote veins and associated dilation/cataclasis. Its upper and lower boundaries dip very shallowly to the SW (Figure 5-33). No cavities or crush zones were observed in the borehole image at this depth interval.

A similar situation is found at depth 224.259 m. The scanned thin section of sample KLX17A-1, taken at that depth, is shown in Figure 5-34. The epidote sealed network is extremely fine grained and is associated with significant localised cataclasis.

Several striated planes were constrained kinematically within DZ 3. Figure 5-35 plots a set of NW and SE dipping reverse and normal fractures (possibly a conjugate set) and a group of much steeper SE-NW-striking and SW-dipping fractures with a component of sinistral and dextral oblique shear.

Figure 5-33. *Minor cataclastic interval and sealed vein network at depth 221.2 in DZ 3 of KLX17A.*

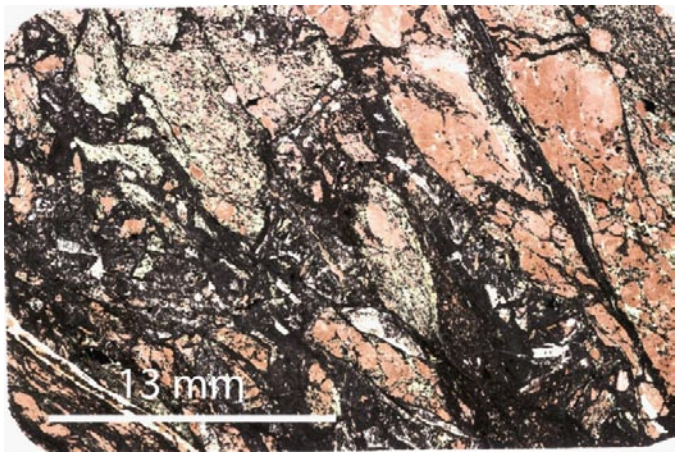

Figure 5-34. *Scanned thin section of sample KLX17A-1. Note the cataclastic texture of the rock and the dense sealed fracture network.*

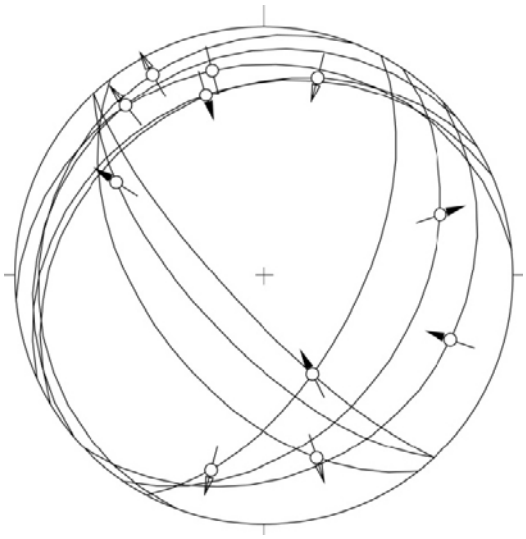

Figure 5-35. *Fault-slip data for DZ 3.*

Table 5-6. Summary of DZ 3.

Depth (m)	Box number	Interpretation	Description
191	25	Host rock	
~199.75			Red staining.
199.966	26	Core	Thin cataclastic fault core.
~200.75	26		Red staining.
~200.75–219	26–30	Host rock	
~219	30		Red staining.
221.211–221.390	30	Core	Dilatant epidote sealed network and cataclasis.
221.390–224.259	30, 31		Red staining, some epidote network.
224.259–224.558	31		Zone of strong epidotization.
224.558–~225.3	31		Red staining.
225.3	31	Host rock	Undeformed rock.

5.5 KLX19A

KLX19A is located in the southwestern corner of the Laxemar investigation area, in a zone dominated at the surface by quartz monzodiorites (Figure 5-1). The drill core is 800.070 m long and is oriented 197/57 /Carlsten et al. 2007d/. We have inspected DZ 4, 5, 6 and 7.

5.5.1 DZ 4: depth interval 436–465 m

DZ 4 is located between 436 and 465 m depth and contains several thin fault cores with no or only minor transition zones (Figure 5-36).

A first upper core starts at depth 448.7 m and extends down to 452.9 m. The core is formed in its upper part by foliated quartz monzonites (Figure 5-37a). In its central sector, at depth 449–449.25 m, it contains a sharp cataclastic interval (Figure 5-37b), which is about 25 cm thick. The stereonet of Figure 5-37 plots the orientation of the ductile fabric (black great circles) and of open fractures within the cataclastic sequence (red circles). Foliation planes and open fractures dip all very steeply to the SE, SSE.

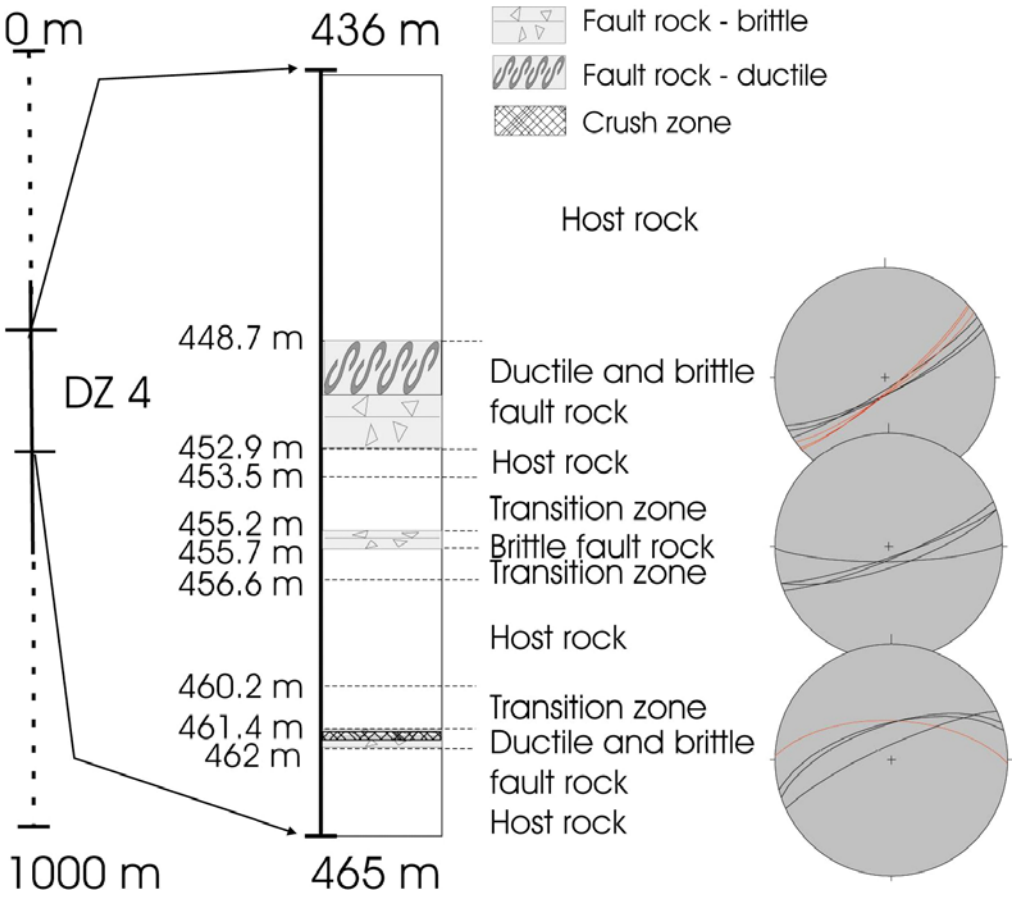

Figure 5-36. *Structural log of DZ 4 in KLX19A. Vertical scale is schematic.*

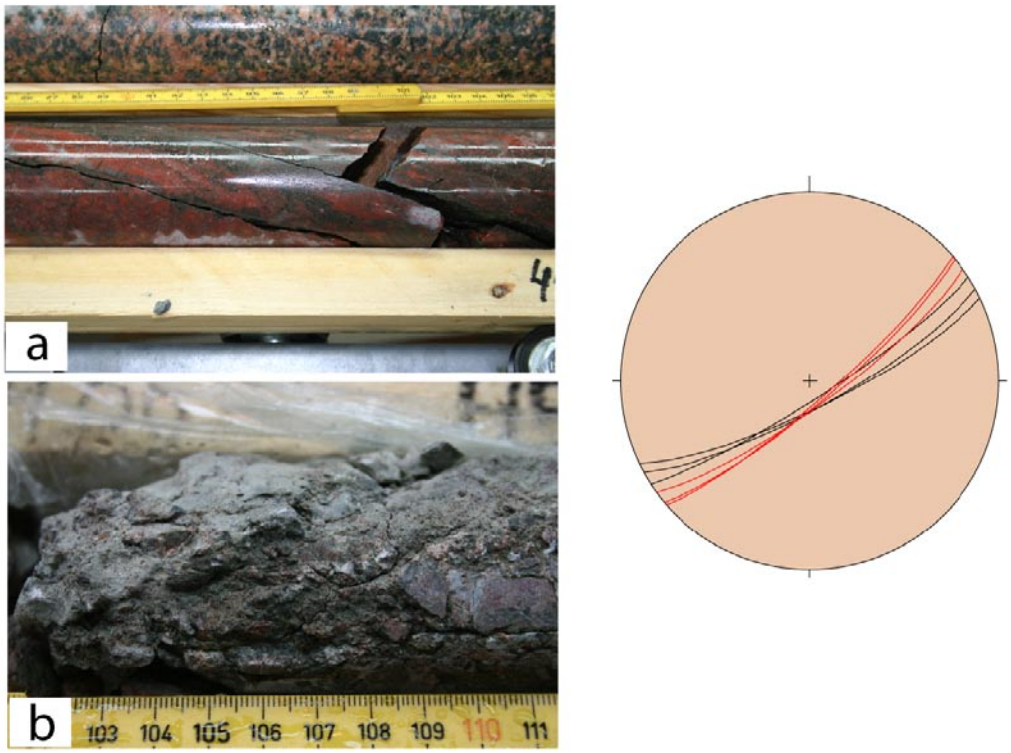

Figure 5-37. *(a) Ductile fabric in the upper part of the DZ core at depth 448.7 m. (b): Cataclastic core at depth 449 m. (c) Orientation of the ductile fabric (black great circles) and of open fractures within the cataclastic interval (red great circles).*

Another brittle core, preceded and followed by two minor transition zones, straddles the depth interval 455.261–455.702 m (Figure 5-38). The core, together with its two transition zones, is a clear example of deformation zone defined on the basis of fracture frequency.

As visible in Figure 5-38, the core resembles in fact a crush zone, and the existence of the core is inferred on the basis of a high fracture frequency rather than on the presence of fault rock. Furthermore, fracture frequency increases progressively towards the core and away from it, thus defining an upper and lower, symmetrically-arranged transition zone. Fractures in the core dip very steeply to the SSE, similarly to the orientation of the upper core described above.

A last core is located at 461.46 m and extends to c. 462 m depth. It is mainly characterised by pervasively foliated quartz monzonites, oriented 272/62 (red great circle in Figure 5-39). A minor crush zone is located in the middle of the ductile interval, between depths 461.585 m and 461.743 m. The ENE-WSW striking black great circles of Figure 5-39 plot the orientation of open fractures associated with the crush zone.

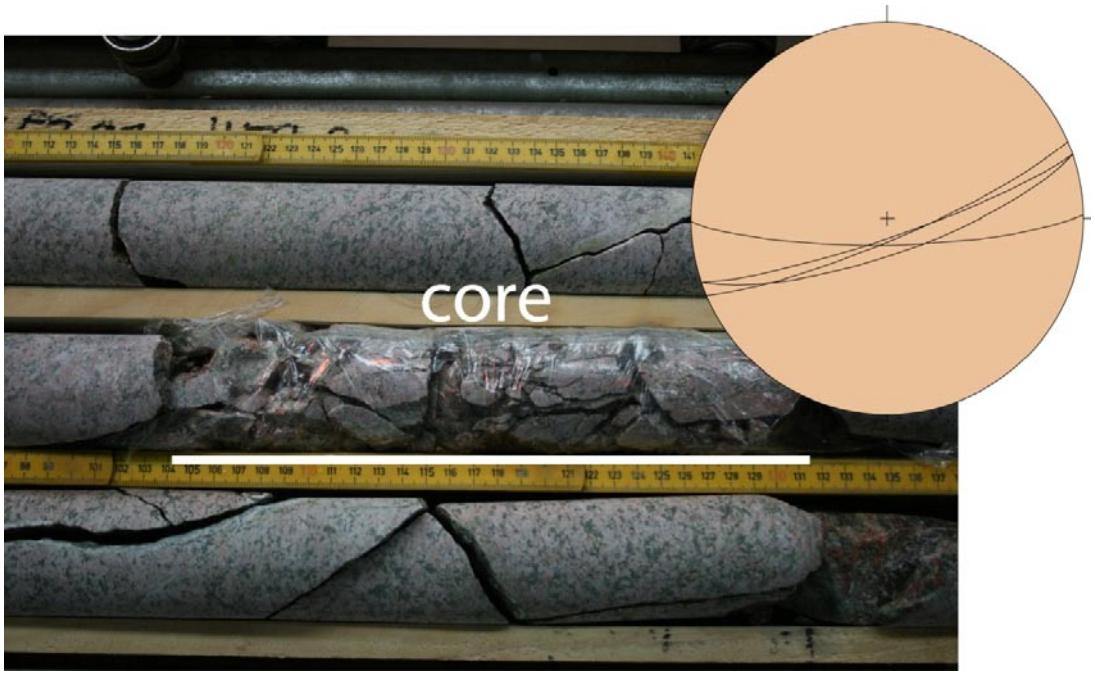

Figure 5-38. *DZ core, defined by a high fracture frequency, extending from 455.261 to 455.702 m depth.*

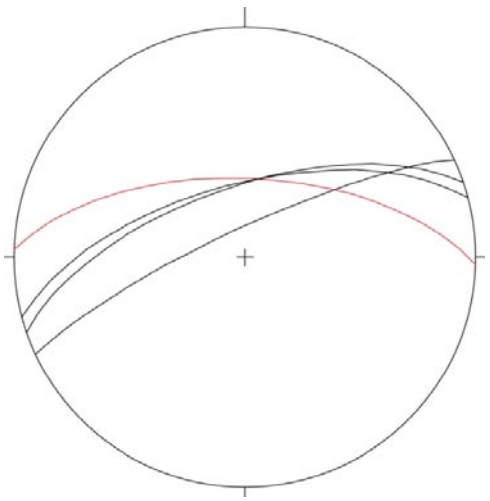

Figure 5-39. *Orientation of the quartz monzonites foliation (red great circle) and of open fractures (black great circles) in the core at depth 461.4 m.*

Table 5-7. Summary of DZ 4.

Depth (m)	Box number	Interpretation	Description
438.5	63–64	Host rock	
448.704–452.988	64	Core	Ductile core overprinted by brittle deformation.
448.704–449			1) Ductile fabric.
449–449.25			2) Cataclasites/breccia.
449.2–452.988			3) Ductile fabric.
452.988–453.56	65–66	Host rock	
453.56–455.261	66	Transition	Increase in fracture frequency.
455.261–455.702	66	Core	Brittle core due to high fracture frequency and loss of cohesion.
455.702–456.64	66	Transition	Decrease in fracture frequency.
456.64–~460.20	66–67	Host rock	
~460.20–461.468	67	Transition	Slight increase in fracture frequency.
461.468–~462	67	Core	Ductile core overprinted by brittle deformation.
461.468–461.585			1) Ductile fabric.
461.585–461.743			2) Brittle crush zone.
461.743– ~462			3) Ductile fabric.
~462	67–68	Host rock	

5.5.2 DZ 5: depth interval 481–508 m

DZ 5 is entirely hosted within a dolerite dyke intruded upon quartz monzonites. The fracture frequency increases significantly within the mafic intrusion up to values well in excess of 9 f/m, which, according to /Munier et al. 2005/, allows the establishment of a DZ core within the dyke (Figure 5-40 and Figure 5-41).

The upper and lower contacts of the dyke are very steep; they are located at 482.6 and 507. 6 m depth and are oriented 202/80 and 343/80, respectively.

A problem, which hampered the gathering of a significant fracture orientation dataset and the characterisation of the DZ kinematics, is the extreme compositional homogeneity of the dolerite, which lacks easily recognizable visual markers. This in turn makes it very difficult to recognize the drill core fractures in the borehole image, thus preventing from their confident orientation. Other unfortunate technical issues affected the characterisation of DZ 5 in KLX19A. The BIPS image length scale is dependent on length adjustments based upon fixed points engraved onto the borehole wall. By counting the drilling rods and measuring the length of the part of the last rod sticking out of the borehole, the position of these fixed points is calculated. In the case of borehole KLX19A, however, the exact position of the marks could not be precisely established. In the lower part of this borehole a mistake was made in the rod counting, which led to a series of faulty positions farther down the borehole. An attempt to correct this error was made, but the accuracy of the recalculated absolute positions is still very low in the deepest part of the borehole. Moreover, the numerous fractures and sections with crush and core loss that characterise this section of the borehole made it almost impossible to identify the same structural feature in the BIPS image and in the core.

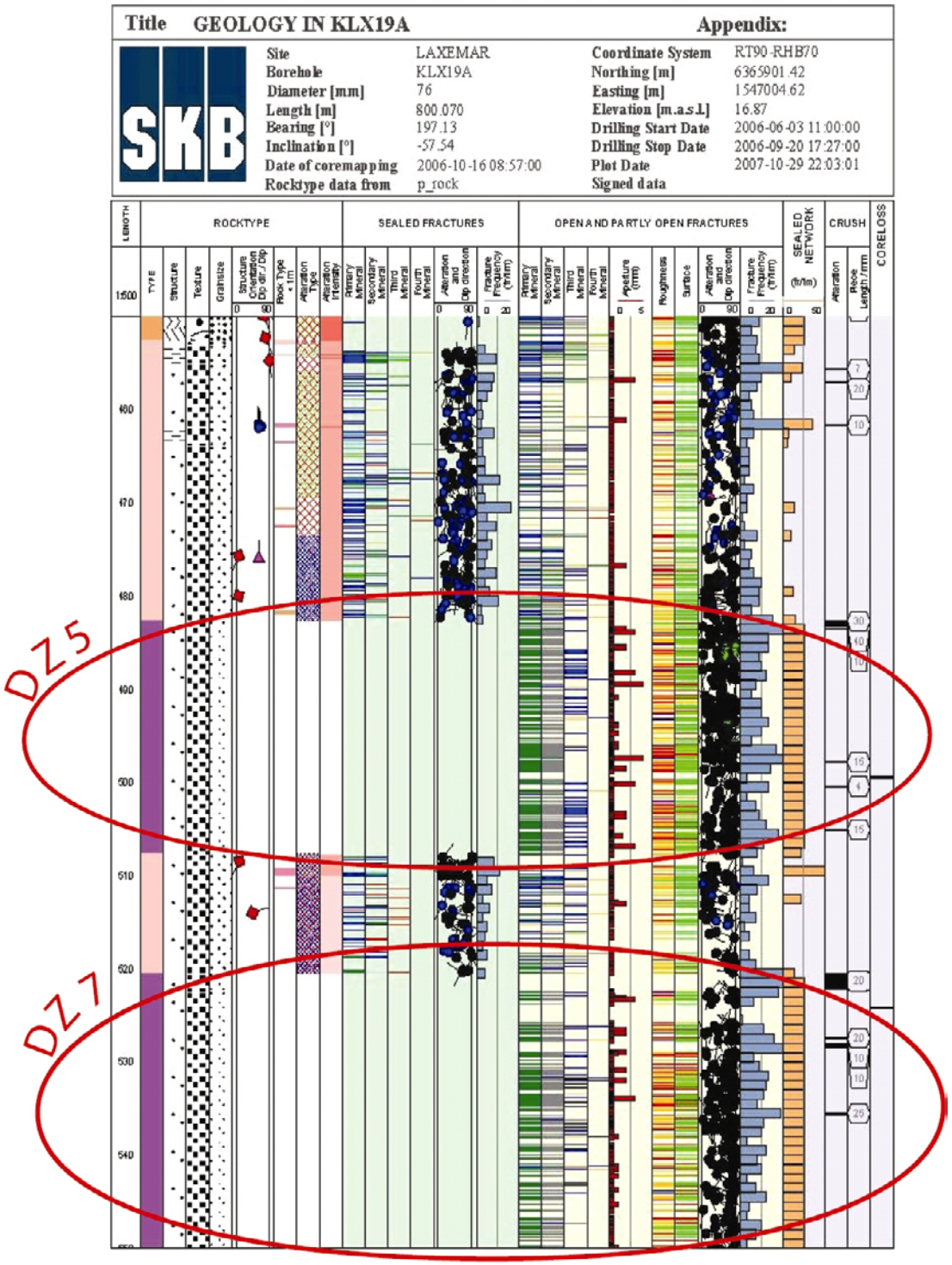

Figure 5-40. *Single-hole data for KLX19A. The red ellipses circle the depth intervals corresponding to DZ 5 and DZ 7. A significant increase in the number of open fractures and sealed networks can be observed within the dolerite dike-hosted DZ's.*

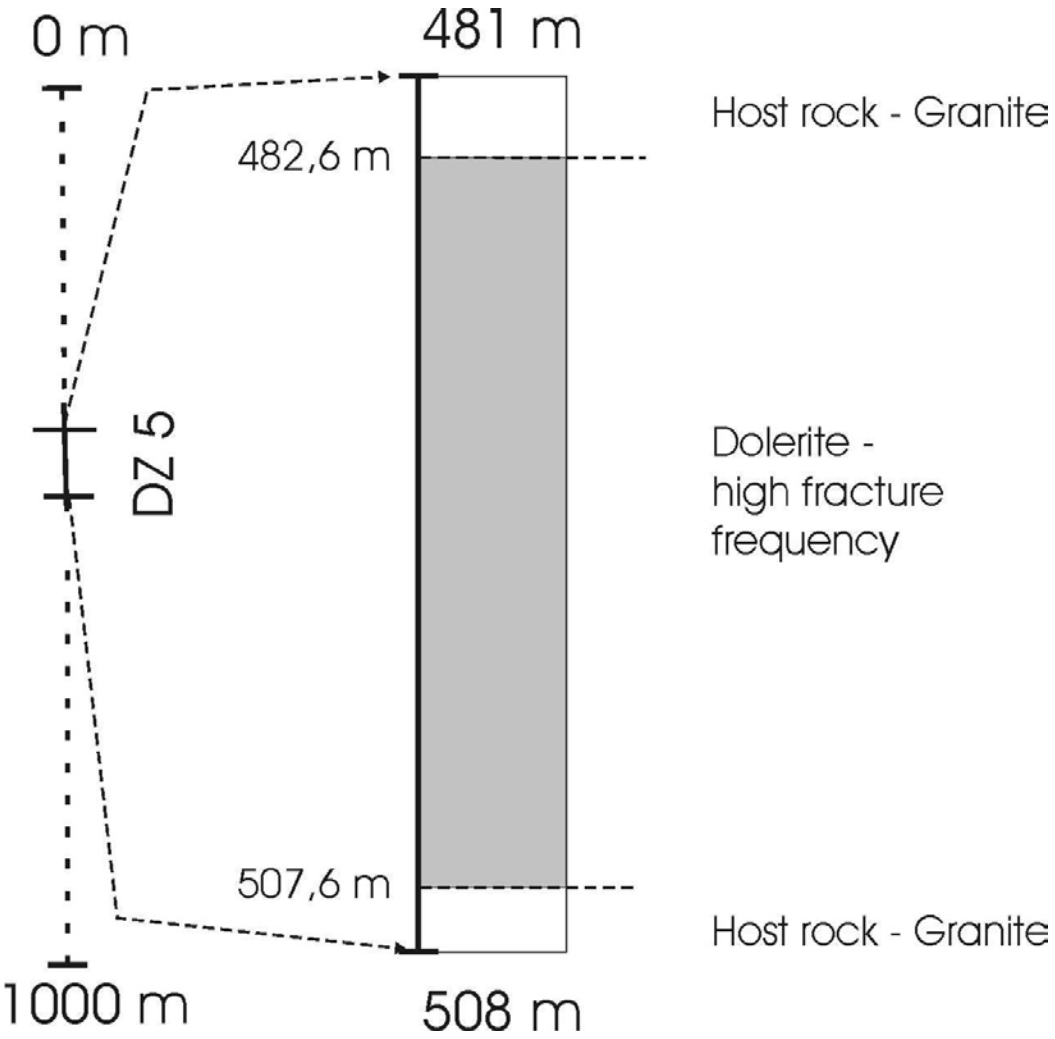

Figure 5-41. *Structural log of DZ 5. The deformation zone is hosted entirely within a dolerite dyke. Vertical scale is schematic.*

Only a very limited number of fracture planes could thus be oriented. Nonetheless, we could recognize and document a very systematic relationship among different fracture generations, whereby low α, steep fractures, usually arranged in anastomosing sealed networks, are cut across, often with visible offsets, by high-α flatter fractures (Figure 5-42).

Normal kinematics were documented for some of the gently dipping fractures (red great circles in the stereonet of Figure 5-42), whereas it was not possible to constrain kinematically the steeper fractures. Chlorite, clay and phrenite are the common coating along these fractures.

Table 5-8. Summary of DZ 5.

Depth (m)	Box number	Interpretation	Description
479–482.603	71	Host rock.	Quartz monzonite.
482.603–507.675	71–76	Lithological change. Core.	Dolerite dyke. Fracture frequency higher than 9 f/m, which allows the definition of a deformation zone core in the dolerite.
507.675–	76	Host rock.	Quartz monzonite.

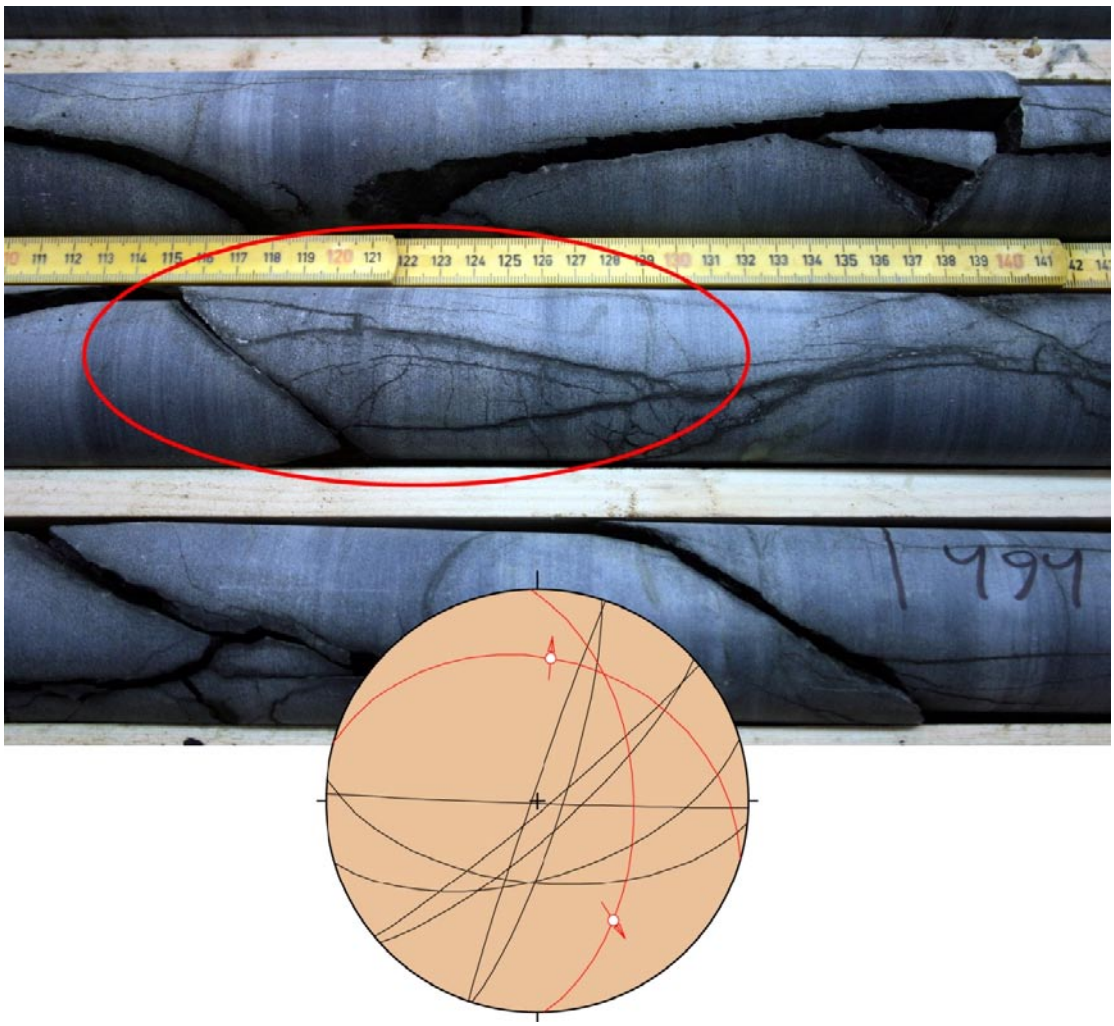

Figure 5-42. *The circled area in the photograph highlights an example of shallow, high α fracture, crosscutting earlier steep, low α fractures. This geometric relationship is commonly observed in DZ 5. The stereonet plots the orientation and normal kinematics of two of these low dip angle fractures (red great circles) and several steeper fractures cut across by the former.*

5.5.3 DZ 6 and 7: depth interval 511–553 m

The depth interval corresponding to DZ 6 does not contain any relevant structural feature and is therefore not classified as a deformation zone.

Similarly to DZ 5, DZ 7 is entirely located within a doleritic dyke (Figure 5-42 and Figure 5-43). The dolerite contains a high fracture density that locally leads to narrow crash zones and minor intervals of core loss. Neither ductile features nor fault rocks were observed.

The granitic host rock contains distinctly less fractures than the dolerite. Numerous fractures and striated planes are observed.

Similarly to DZ 5, the characterisation of DZ7 was not possible for the same technical issues that made impossible a structural/kinematic interpretation of DZ 5.

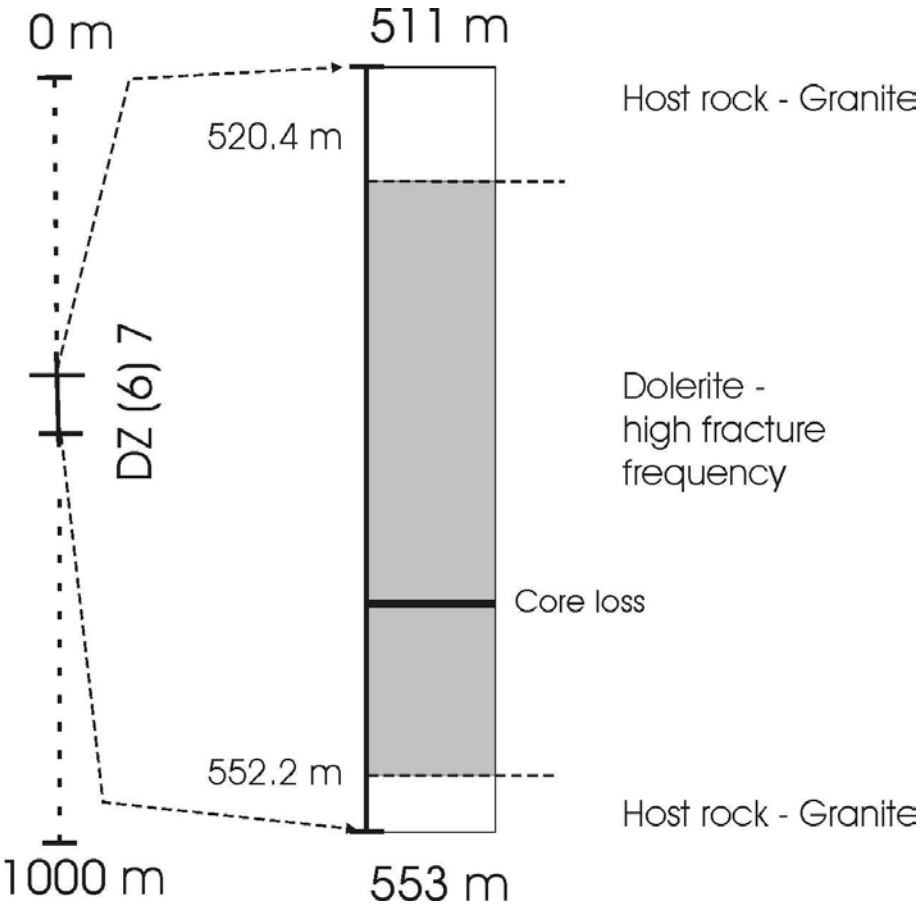

Figure 5-43. *Log for DZ 7 of KLX19, hosted within a dolerite dyke extending from 520 down to 552 m depth. Vertical scale is schematic.*

Table 5-9: Summary of DZ 6 and 7.

Depth (m)	Box number	Interpretation	Description
511–520.437	77–78	Host rock	Undeformed granitic rock.
520.437	78	Lithological change	
520.437–552.213	78–84		Dolerite dyke, with high fracture frequency.
	79		13 cm core loss.
	80		12 cm core loss
552.213	84	Lithological change	
552.213–	84	Host rock	Undeformed granitic rock.

5.6 KLX21B

KLX21B is located in the easternmost sector of the Laxemar investigation area, in a zone dominated at the surface by the Ävro granite to monzodiorite (Figure 5-1). We have inspected DZ 12.

5.6.1 DZ 12: depth interval 594–707 m

DZ 12 extends from 594 to 707 m depth and within this depth interval the borehole is oriented 223/68 /Carlsten et al. 2008b/ (Figure 5-44). The zone is hosted within a porphyritic, medium-grained granite to quartz monzodiorite.

No significant structural features were observed and we do not classify DZ 12 as a proper deformation zone, because it does not fulfill the general structural criteria discussed in the introduction of this report. It lacks a proper core and transition zones.

Nonetheless, a few minor structures are present within the logged interval and are reported here.

At 606.56 m depth, for example, there is a. c. 50 cm thick ductile, pervasively foliated sequence. Mylonitic foliation dips very shallowly to the west (Figure 5-45).

The thin shear zone presents gradational contacts to the equigranular texture of the granite and does not display any sign of brittle overprinting.

At depth 618.09 m there is a crush zone. BIPS images allowed the measurement of one of its main fractures, oriented 180/58 (Figure 5-46). The crush zone formed at the expense of a dilatant sealed network containing veins of calcite, epidote and clay minerals (Figure 5-46). Dilation led to localised, minor brecciation.

A similar example of sealed dilatant calcite-epidote network is found at depth 625.74 (Figure 5-47).

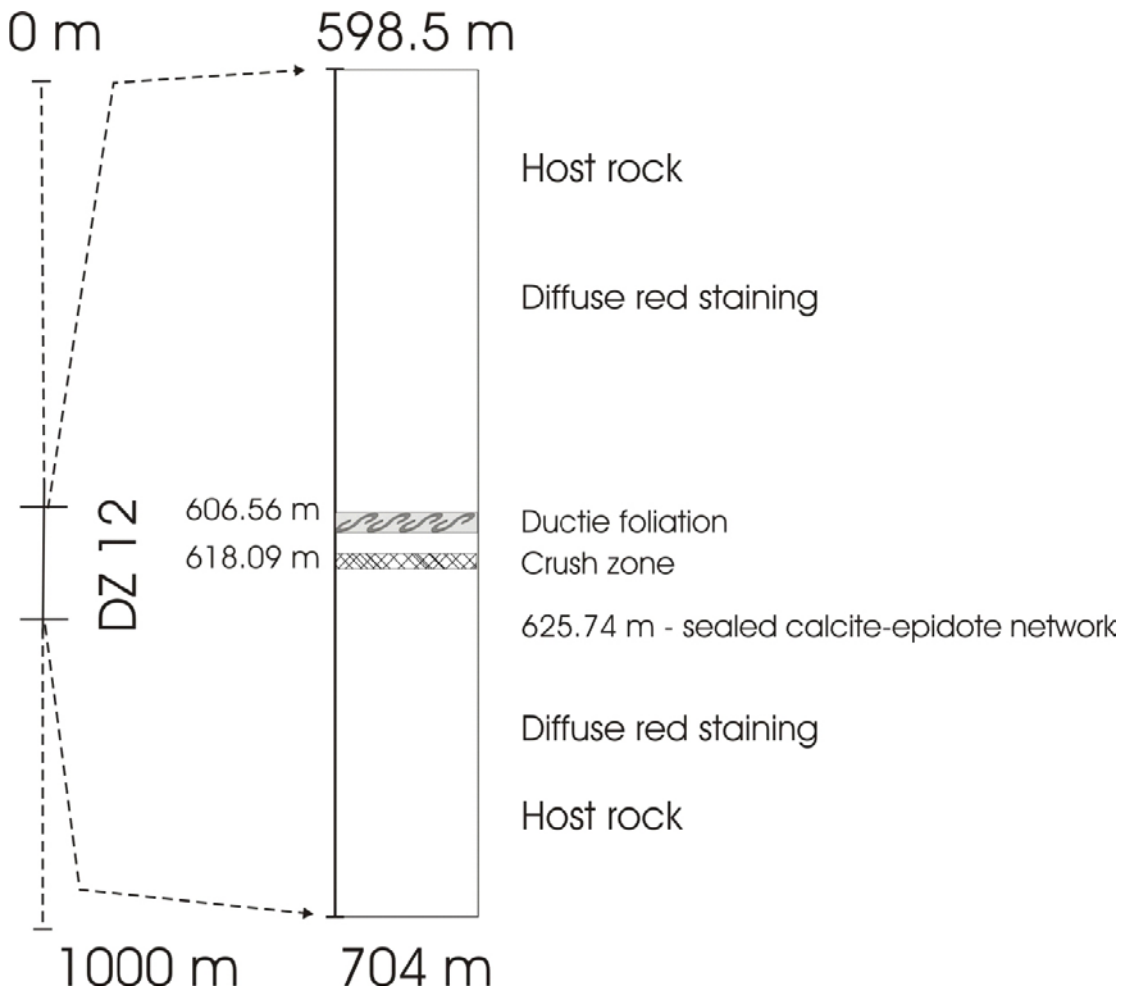

Figure 5-44. *Structural log of DZ 12. Vertical scale is schematic.*

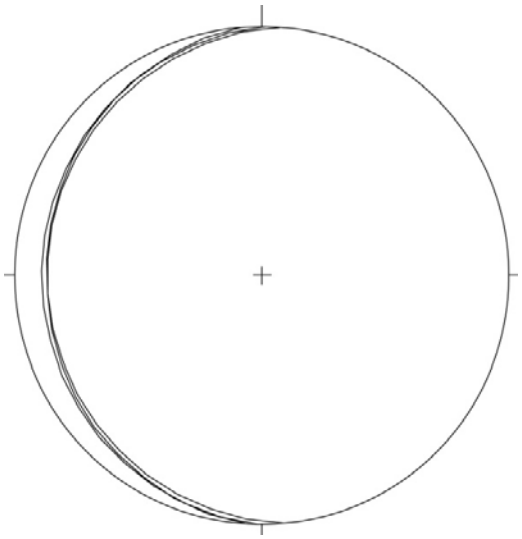

Figure 5-45. *Shallow, W-dipping foliation planes characterise a thin mylonitic interval extending from 606.56 to 607.2 m depth.*

Figure 5-46. *Thin crush zone and orientation of one of its main fractures at depth 618.090 m.*

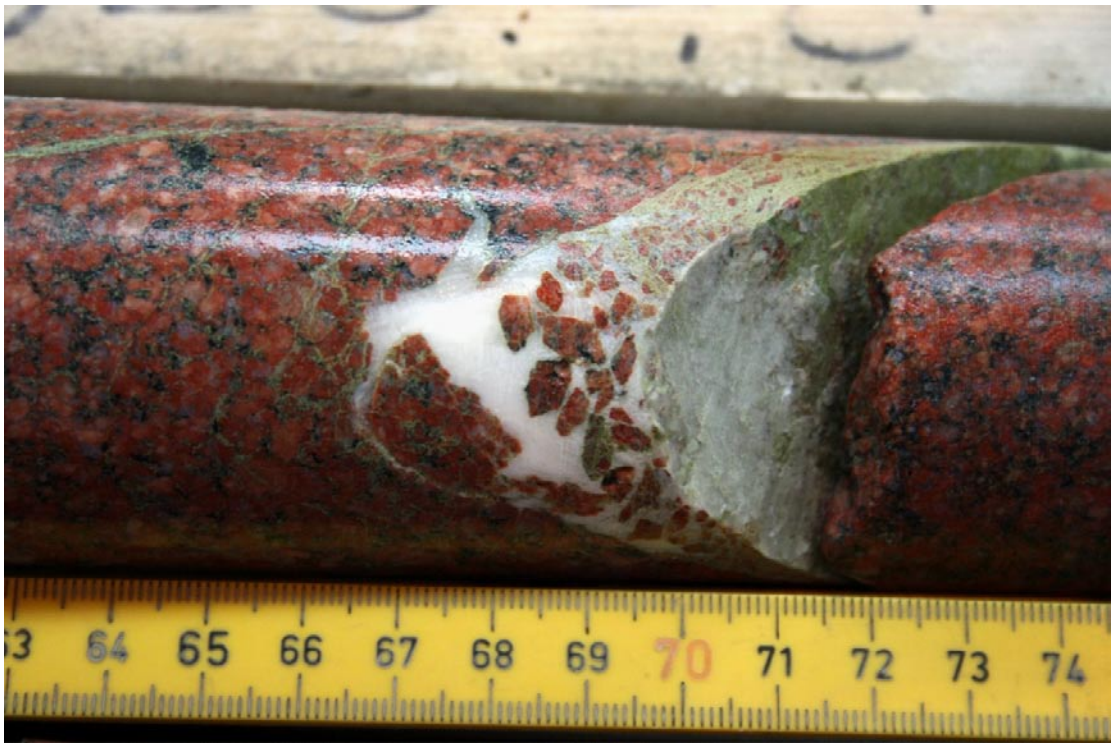

Figure 5-47. *Dilatant epidote-calcite vein. Crosscutting relationships suggest the calcite to postdate epidotization.*

Here, crosscutting relationships and the fact that epidote clasts are reworked within calcite veins, suggest that calcite veining is the last step of a complex dilational and veining history. This structural relationship is common throughout DZ 12 of KLX21B (see also the examples of Figure 5-48).

Several striated planes are contained in the DZ. They are coated invariably by epidote, chlorite and calcite (Figure 5-49). Although the kinematics of several surfaces could not be determined, slickensided planes dip gently to moderately to the SW, W and NW. High obliquity reverse and normal senses of shear are frequent (Figure 5-49).

Red staining is pervasive throughout the DZ. Fracture frequency is in general low (2–5 f/m), but it increases significantly in the last 4–5 m of the deformation zone.

Figure 5-48. *Typical crosscutting relationships in DZ 12 of KLX21B between earlier epidote networks and subsequent calcite veins. As shown very clearly by the bottom photograph, calcite veining was locally associated with significant dilation. Large clasts of the host rock (containing evidence of earlier epidotization along discrete fractures) were ripped off and rotated within the space created at the time of injection of calcite.*

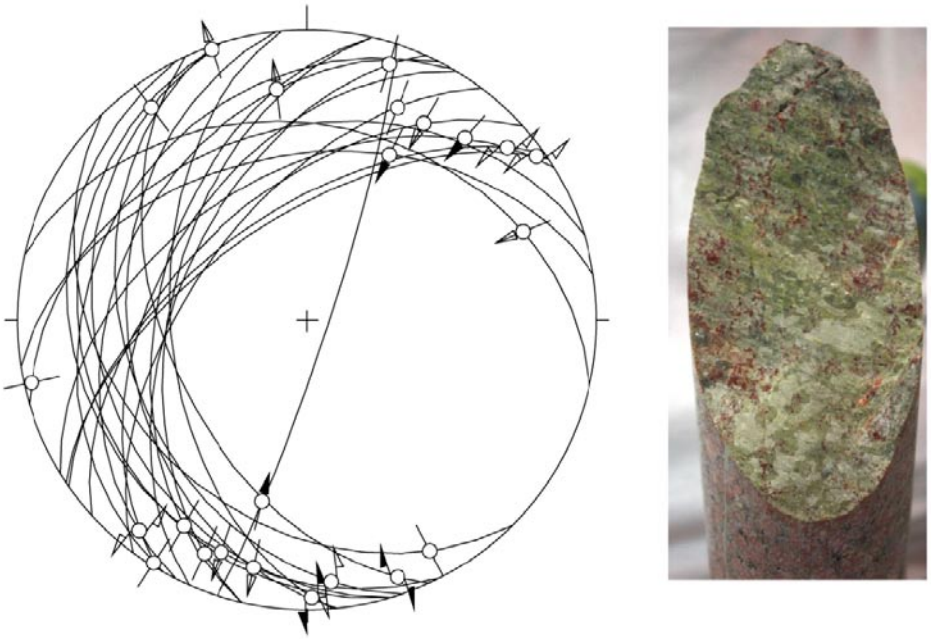

Figure 5-49. *Striated surfaces in DZ 12 of KLX21B dip gently to moderately to the SW, W and NW. High obliquity (thus transtensional and transpressional) normal and reverse shear is observed on most of the fracture planes. These are coated predominantly by epidote, chlorite and calcite.*

6 References

Braathen A, 1999. Kinematics of brittle faulting in the Sunnfjord region, western Norway. Tectonophysics 302, 99–121.

Braathen A, Gabrielsen R H, 2000. Bruddsoner i fjell – oppbygning og definisjoner. Gråstein, 7, 1–20. Norges geologiske undersøkelse, ISSN 0807-4801.

Braathen A, Osmundsen P T, Nordgulen Ø, Roberts D, Meyer G B, 2002. Orogen-parallel extension of the Caledonides in northern Central Norway: an overview. Norwegian Journal of Geology, 82, 225–241.

Braathen A, Osmundsen P T, Gabrielsen R, 2004. Dynamic development of fault rocks in a crustal-scale detachment; an example from western Norway. Tectonics, 23, TC4010, doi:10.1029/2003TC001558.

Caine J S, Evans J P, Forster C B, 1996. Fault zone architecture and permeability structure. Geology, 24, 11, 1025–1028.

Carlsten S, Hultgren P, Mattsson H, Stanfors R, Stråhle A, Wahlgren C-H, 2007a. Geological single-hole interpretation of KLX13A, HLX39 and HLX41. SKB P-07-15. Svensk Kärnbränslehantering AB.

Carlsten S, Curtis P, Hultgren P, Mattsson H, Mattsso K-J, Stråhle A, Whalgren C-H, 2007b. Geological single-hole interpretation of KLX16A. SKB P-07-208. Svensk Kärnbränslehantering AB.

Carlsten S, Hultgren P, Mattsson H, Mattsso K-J, Stråhle A, Whalgren C-H, 2007c. Geological single-hole interpretation of KLX17A and HLX42. SKB P-07-209. Svensk Kärnbränslehantering AB.

Carlsten S, Hultgren P, Mattsson H, Mattsso K-J, Stråhle A, Whalgren C-H, 2007d. Geological single-hole interpretation of KLX19A and HLX38. SKB P-07-161. Svensk Kärnbränslehantering AB.

Carlsten S, Hultgren P, Mattsson H, Mattsson K H, Stråhle A, Wahlgren C-H, 2008a. Geological single-hole interpretation of KLX15A, HLX30, HLX31 and HLX33. SKB P-08-05. Svensk Kärnbränslehantering AB.

Carlsten S, Curtis P, Mattsson K H, Stråhle A, Thunehed H, Wahlgren C-H, 2008b. Geological single-hole interpretation of KLX21B and HLX40. SKB P-08-06. Svensk Kärnbränslehantering AB.

Evens J P, Forster C B, Goddard J V, 1997. Permeability of fault-related rocks, and implications for hydraulic structure of fault zones. Journal of Structural Geology, 19, 1393–1404.

Gudmundsson A, Berg S S, Lyslo K B, Skurtveit E, 2001. Fracture networks and fluid transport in active fault zones. Journal of Structural Geology 23, 343–353.

Munier R, Stanfors R, Milnes A G, Hermanson J, Triumf C-A, 2003. Geological Site Descriptive Model. A strategy for the development during site investigations. SKB R-03-07. Svensk Kärnbränslehantering AB.

Nordgulen Ø, Braathen A, Corfu F, Osmundsen P T, Husmo T, 2002. Polyphase kinematics and geochronology of the Kollstraumen detachment, north-central Norway. Norwegian Journal of Geology, 82, 299–316.

Osmundsen P T, Braathen A, Nordgulen Ø, Roberts D, Meyer G B, Eide E A, 2003. The Nesna shear zone and adjacent gneiss-cored culminations, North-central Norwegian Caledonides. Journal of the Geological Society, London 160*,* 1–14.

Petit J P, 1987. Criteria for the sense of movement on fault surfaces in brittle rocks. Journal of Structural Geology 9, 597–608.

Viola G, Venvik Ganerød G, 2007a. Structural analysis of brittle deformation zones in the Simpevarp-Laxemar area, Oskarshamn, southeast Sweden. SKB P-07-41. Svensk Kärnbränslehantering AB.

Viola G, Venvik Ganerød G, 2007b. Structural characterisation of deformation zones (faults and ductile shear zones) from selected drill cores and outcrops from the Laxemar area – Results from Phase 2. In press. Svensk Kärnbränslehantering AB.

Appendix

Cores and core sections logged

Drill core	DZ	Sec up (m)	Sec low (m)	Metres
KLX 13 A	DZ 7	487	594	107
KLX 15A	DZ 16	711	744	33
	DZ 20	978	1,000	22
KLX 16A	DZ 12	325	435	110
KLX 17A	DZ 1	100	114	14
	DZ 3	192	228	36
KLX 19A	DZ 4	436	465	29
	DZ 5	481	508	27
	DZ 7	520	553	33
KLX 21B	DZ 12	594	707	113
Totalt				524